Small but strong: A review of the mechanical properties of carbon nanotube–polymer composites

Article *in* Carbon · August 2006

DOI: 10.1016/j.carbon.2006.02.038

4 authors, including:

Jonathan Coleman
Trinity College Dublin
219 PUBLICATIONS **20,198** CITATIONS
SEE PROFILE

Umar Khan
Trinity College Dublin
48 PUBLICATIONS **7,515** CITATIONS
SEE PROFILE

Werner J Blau
Trinity College Dublin
588 PUBLICATIONS **19,016** CITATIONS
SEE PROFILE

Available online at www.sciencedirect.com
SCIENCE DIRECT
Carbon 44 (2006) 1624–1652
CARBON
www.elsevier.com/locate/carbon

Small but strong: A review of the mechanical properties of carbon nanotube–polymer composites

Jonathan N. Coleman [a,*], Umar Khan [a], Werner J. Blau [a], Yurii K. Gun'ko [b]

[a] School of Physics, Trinity College Dublin, Dublin 2, Ireland
[b] School of Chemistry, Trinity College Dublin, Dublin 2, Ireland

Received 24 October 2005; accepted 23 February 2006

Abstract

The superlative mechanical properties of carbon nanotubes make them the filler material of choice for composite reinforcement. In this paper we review the progress to date in the field of mechanical reinforcement of polymers using nanotubes. Initially, the basics of fibre reinforced composites are introduced and the prerequisites for successful reinforcement discussed. The effectiveness of different processing methods is compared and the state of the art demonstrated. In addition we discuss the levels of reinforcement that have actually been achieved. While the focus will be on enhancement of Young's modulus we will also discuss enhancement of strength and toughness. Finally we compare and tabulate these results. This leads to a discussion of the most promising processing methods for mechanical reinforcement and the outlook for the future.

Keywords: Carbon nanotubes; Mechanical properties; Carbon composites

Contents

* Corresponding author. Tel.: +353 16083859; fax: +353 16711759.
E-mail address: colemaj@tcd.ie (J.N. Coleman).

0008-6223/$ - see front matter © 2006 Elsevier Ltd. All rights reserved.
doi:10.1016/j.carbon.2006.02.038

1. Introduction

Since their discovery in 1991, carbon nanotubes have generated huge activity in most areas of science and engineering due to their unprecedented physical and chemical properties. No previous material has displayed the combination of superlative mechanical, thermal and electronic properties attributed to them. These properties make nanotubes ideal, not only for a wide range of applications [1] but as a test bed for fundamental science [2].

In particular, this combination of properties makes them ideal candidates as advanced filler materials in composites. Researchers have envisaged taking advantage of their conductivity and high aspect ratio to produce conductive plastics with exceedingly low percolation thresholds [3]. In another area, it is thought that their massive thermal conductivity can be exploited to make thermally conductive composites [4]. However, probably the most promising area of composites research involves the mechanical enhancement of plastics using carbon nanotubes as reinforcing fillers.

The idea of using pseudo one-dimensional fillers as a reinforcing agent is nothing new: straw has been used to reinforce mud bricks since about 4000 BC. In more recent times, fibres made from materials such as alumina, glass, boron, silicon carbide and especially carbon have been used as fillers in composites. However, these conventional fibres have dimensions on the meso-scale with diameters of tens of microns and lengths of order of millimetres. Their mechanical properties are impressive with carbon fibres typically displaying stiffness and strength in the ranges 230–725 GPa and 1.5–4.8 GPa, respectively [5]. In recent years carbon nanofibres have been grown from the vapor phase with diameters of order of 100 nm and lengths between 20 and 100 μm. These small dimensions mean they have much higher surface area per unit mass than conventional carbon fibres allowing much greater interaction with composite matrices. They also tend to have impressive mechanical properties with Young's modulus in the range 100–1000 GPa and strengths between 2.5 and 3.5 GPa [6].

However the ultimate mechanical filler material must be carbon nanotubes. Nanotubes can have diameters ranging from 1 to 100 nm and lengths of up to millimetres [7]. Their densities can be as low as $\sim$1.3 g/cm^3 and their Young's moduli are superior to all carbon fibres with values greater than 1 TPa [8]. However, their strength is what really sets them apart. The highest measured strength for a carbon nanotube was 63 GPa [9]. This is an order of magnitude stronger than high strength carbon fibres. Even the weakest type of carbon nanotubes have strengths of several GPa [10].

However a large amount of work will have to be done before we can really make the most of the exceptional mechanical properties of carbon nanotubes. In this paper we will explore the progress that has already been made to this end. First we will review the properties of carbon nanotubes and the theory of fibre reinforcement. This will lead us to a study of the system requirements in order to achieve reinforcement. The techniques used in the literature to produce polymer–nanotube composites will be reviewed before we look at what levels of reinforcements have actually been achieved. Finally we will discuss the advances made so far and study what needs to be done in the future.

2. Properties of nanotubes

There are two main types of nanotubes available today. Single walled nanotubes (SWNT) [11,12] consist of a single sheet of graphene rolled seamlessly to form a cylinder with diameter of order of 1 nm and length of up to centimetres. Multi-walled nanotubes (MWNT) consist of an array of such cylinders formed concentrically and separated by 0.35 nm, similar to the basal plane separation in graphite [13]. MWNTs can have diameters from 2 to 100 nm and lengths of tens of microns.

Single walled nanotubes can be fabricated in a variety of ways. Early fabrication relied on a modified version of

arc-discharge generators used for Fullerene synthesis [11,12]. However, today the most common synthetic methods are based on laser ablation [14] and chemical vapor deposition [15,16], in particular, decomposition of CO [17]. It should be noted that, while high quality SWNTs can be produced, some defects are always present. These may significantly affect the physical and chemical properties of the nanotubes.

A graphene sheet may be rolled up in many ways to form a single walled nanotube. The rolling action breaks the symmetry of the planar system and imposes a distinct direction with respect to the hexagonal lattice, the axial direction. Depending on the relationship between this axial direction and the unit vectors describing the hexagonal lattice, the tube can be metallic, semi-metallic or semi-conducting. Semi-conducting nanotubes have bandgaps that scale inversely with diameter, ranging from approximately 1.8 eV for very small diameter tubes to 0.18 eV for the widest possible stable SWNT [18].

Pristine carbon nanotubes are extremely conductive. Due to their one-dimensional nature, charge carriers can travel through nanotubes without scattering resulting in ballistic transport. The absence of scattering means that Joule heating is minimised so that nanotubes can carry very large current densities of up to 100 MA/cm^2 [19]. In addition, carrier mobilities as high as 10^5 cm^2/Vs have been observed in semi-conducting nanotubes [20]. Superconductivity has also been observed in SWNT, albeit with transition temperatures of 5 K [21].

Nanotubes are also very conductive for phonons. Theory predicts a room temperature thermal conductivity of up to 6000 W/m K [22–24]. While this has not yet been attained, values around 200 W/m K have been measured [25].

However, it should be pointed out that pristine, isolated SWNT are rarely available to experimentalists. Due to their great flexibility and high surface energy, SWNT tend to aggregate into large bundles. Bundles contain huge numbers of both metallic and semi-conducting SWNT in a random mixture. Bundle properties are generally inferior to those of isolated SWNT. It is extremely difficult to separate SWNT from bundles making this issue a serious hurdle in the way of real applications.

Well-graphitised, relatively defect free MWNT can be produced by the arc discharge method [26]. In some ways, these materials are rather similar to those of perfect SWNT as the interwall coupling is relatively weak. Electronically, they act as either metals or very small bandgap semi-conductors. Ballistic conduction has been observed by a number of groups [27] and thermal conductivities as high as 3000 W/m K have been measured [28].

However, the most common production mechanism for MWNT is undoubtedly chemical vapor deposition (CVD). Nanotubes made from this method generally have very large quantities of defects. This means their structure is very far from the ideal rolled up hexagonal lattice. Their physical properties suffer due to the presence of defects with thermal, electronic and mechanical properties deviating significantly from those expected for pristine nanotubes. However CVD produced MWNT are important because they can be produced in very large quantities relatively cheaply. If nanotubes are ever to be useful at an industrial level it is likely that they will be produced by some type of CVD process.

2.1. Mechanical properties of nanotubes

From virtually the moment nanotubes were discovered it was expected that they would display superlative mechanical properties by analogy with graphite. It had long been known that graphite had an in-plane modulus of 1.06 TPa [29] and nanotubes were expected to display similar stiffness. While the tensile strength of graphite was not accurately known, Perepelkin had estimated it to be as high as 130 GPa from the properties of C–C bonds [30]. In addition Bacon had fabricated graphite whiskers in 1960 with a yield strength of 20 GPa [31]. Thus, it was expected that carbon nanotubes would be in a class of their own in terms of high strength and stiffness.

Long before sufficient quantities of nanotubes were produced to allow mechanical measurements, a number of studies had used computer simulation to study their properties. As early as 1993, Overney et al. [32] calculated the rigidity of short SWNT using ab initio local density calculations to determine the parameters in a Keating potential. The calculated Young's modulus was 1500 GPa, similar to that of graphite. This was followed by a range of papers predicting that the Young's modulus of nanotubes was close to 1 TPa independent of nanotube type and diameter [33].

The first actual mechanical measurements were made on multi-walled nanotubes produced by the arc discharge process. As only small amounts were available, early measurements were carried out in a transmission electron microscope. Treacy et al. [34] measured the amplitude of intrinsic thermal vibrations observed in the TEM. They used this to calculate moduli of 0.41–4.15 TPa for a number of tubes. Three years later Poncheral induced electromechanical resonant vibrations, giving moduli values between 0.7 and 1.3 TPa [35]. In addition, Falvo et al. observed the reversible bending of MWNT with radii of curvature as low as ~25 nm indicating unprecedented flexibility [36].

The first direct measurement was made by Wong et al. in 1997 [8]. They used an atomic force microscope (AFM) to measure the stiffness constant of arc-MWNTs pinned at one end. This gave an average value for Young's modulus of 1.28 TPa. More importantly they also managed to make the first strength measurements, obtaining an average bending strength of 14 GPa. Salvetat et al. used an AFM to bend an arc-MWNT that had been pinned at each end over a hole [37] obtaining an average modulus value of 810 GPa.

However, the ultimate measurements were carried out by Yu et al. in 2000 when they managed to do stress–strain measurements on individual arc-MWNTs inside an electron microscope [9] (Fig. 1). For a range of tubes they obtained modulus values of 0.27–0.95 TPa. More interestingly they

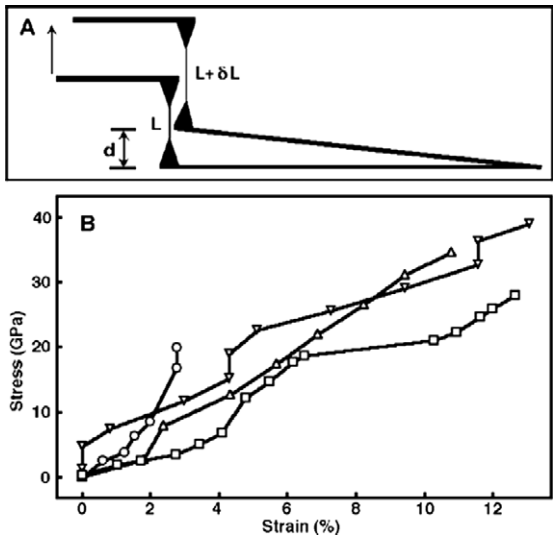

Fig. 1. Stress–strain curves for individual MWNT. Reproduced from [9].

showed fracture of MWNT at strains of up to 12% and with strengths in the range 11–63 GPa. This allows the estimation of nanotube toughness at ~1240 J/g. In addition, failure was observed at the outer tube with the inner walls telescoping out in a "sword and sheath" mechanism.

Measurements on SWNT took longer due to the difficulties in handling them. The first measurements were carried out by Salvetat et al. using their AFM method [38]. They observed a tensile modulus of ~1 TPa for small diameter SWNT bundles by bending methods. However, the properties of larger diameter bundles were dominated by shear slippage of individual nanotubes within the bundle. Yu et al. were able to measure the tensile properties of bundles by the same method they used for their MWNT study. They saw moduli in the range 0.32–1.47 TPa and strengths between 10 and 52 GPa. Failure occurred at a maximum strain of 5.3% giving a toughness of approximately 770 J/g. In addition they observed that failure occurred for the nanotubes on the perimeter of the bundle only with the rest of the tubes slipping apart [39].

Intertube slippage within bundles presents a serious limitation to their mechanical properties. The low shear modulus means that effective moduli and strengths for bundles are far below those expected for individual SWNT. As mentioned previously, it is extremely difficult to de-bundle SWNT. Forro and co-workers showed that SWNT could be fused together in bundles by electron irradiation [40,41]. By fine-tuning the dose and irradiation energy they found that they could increase the bundle bending modulus to 750 GPa, close to that of an individual SWNT.

The relatively high values of modulus and strength values of ~1 TPa and tens of GPa have been measured on high quality SWNT and arc discharge MWNT. However as discussed previously, CVD-MWNT are expected to display significantly reduced values. The first measurements

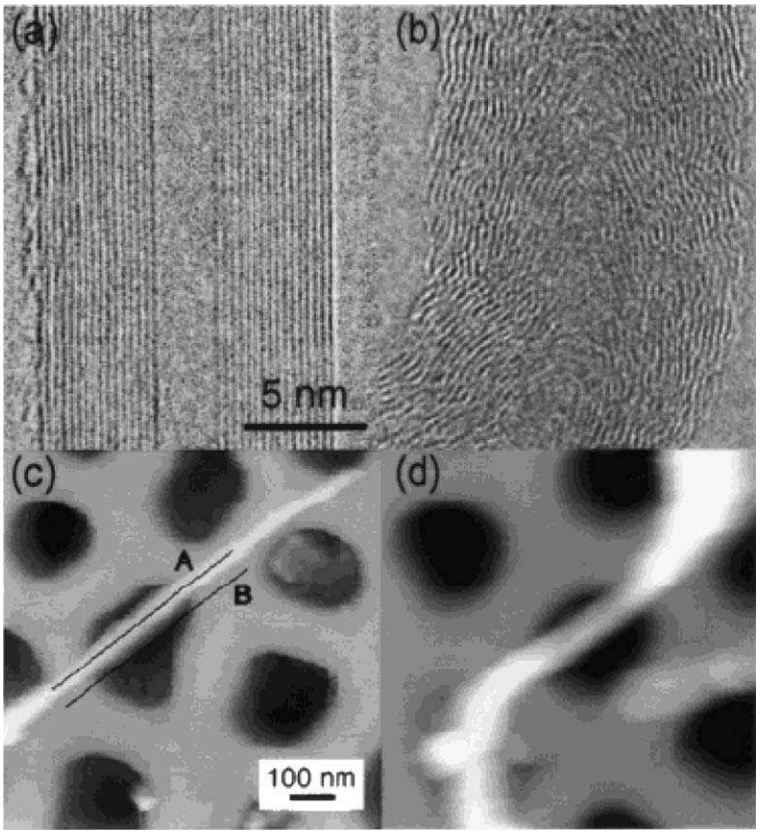

Fig. 2. TEM images of (a) an arc-MWNT, (b) a CVD-MWNT. AFM images of (c) arc-MWNT and (d) CVD-MWNT lying across a pore. Reproduced from [37].

on CVD-MWNT were carried out by Salvetat et al. using the AFM technique (Fig. 2). They measured Young's modulus values between 12 and 50 GPa [37]. Shortly afterwards Xie et al. made stress–strain measurements on bundles of CVD-MWNT [10]. They measured a modulus of 0.45 TPa and values of tensile strength of ~4 GPa. The much larger variation in modulus for CVD-MWNT compared to arc-MWNT strongly suggests that the modulus is very sensitive to defect concentration and type.

3. Theory of fibre reinforced composite materials

A great deal of theoretical work has been carried out since the 1950s with the aim of modelling the mechanical properties of fibre reinforced composites. While some of these models [42] are quite sophisticated, we will consider two of the simplest and most common. These are the rule of mixtures and the Halpin–Tsai equations.

In the simplest possible case a composite can be modelled as an isotropic, elastic matrix filled with aligned elastic fibres that span the full length of the specimen. We assume that the matrix and fibres are very well-bonded. Then, on application of a stress in the fibre alignment direction, the matrix and fibres will be equally strained. Under these circumstances, the composite tensile modulus in the alignment direction, Y_C, is given by

$$Y_C = (Y_f - Y_m)V_f + Y_m \quad (1)$$

where Y_f is the fibre modulus, Y_m is the matrix modulus and V_f is the fibre volume fraction. This is the well-known rule of mixtures [5].

However, this describes a rather idealised situation, fibres are generally much shorter than the specimen length. For short fibres we must consider the matrix–fibre stress transfer. When the matrix is under stress, the maximum stress transferred to the fibre is described by the interfacial stress transfer, τ. The stress transferred scales with fibre length, l, so that at some critical length, l_c, the stress transferred is large enough to break the fibre. For a hollow cylinder, this critical length is given by

$$l_c = \frac{\sigma_f D}{2\tau}\left[1 - \frac{D_i^2}{D^2}\right] \quad (2)$$

where σ_f is the fibre strength, D and D_i are the fibre external and internal diameters, respectively [43].

In effect, the stress transferred to the fibre builds up to its maximum value (σ_f, that which causes breakage) over a distance l_c from the end of the fibre. This means that short fibres carry load less efficiently than long fibres meaning that they can be thought of as having a lower effective modulus for reinforcement purposes. This was first considered by Cox [44] who showed that for aligned fibres the composite modulus is given by

$$Y_C = (\eta_l Y_f - Y_m)V_f + Y_m \quad (3)$$

where η_l is the length efficiency factor, which is described by [45]:

$$\eta_l = 1 - \frac{\mathrm{Tanh}(a \cdot l/D)}{a \cdot l/D} \quad (4)$$

with

$$a = \sqrt{\frac{-3Y_m}{2Y_f \ln V_f}} \quad (5)$$

The length efficiency factor approaches 1 for $l/D > 10$, underlining the fact that high aspect ratio fillers are preferred.

In many situations the fibres may not be aligned. For non-aligned, short fibres, the composite modulus is given by

$$Y_C = (\eta_o \eta_l Y_f - Y_m)V_f + Y_m \quad (6)$$

where η_o is the orientation efficiency factor. This has values of $\eta_o = 1$ for aligned fibres, $\eta_o = 3/8$ for fibres aligned in plane and $\eta_o = 1/5$ for randomly oriented fibres [46].

A similar calculation can be used to derive an equation for composite strength. For very long aligned fibres ($l > \sim 10 l_c$), the composite strength is described by

$$\sigma_C = (\sigma_f - \sigma_m)V_f + \sigma_m \quad (7)$$

where σ_C, σ_f and σ_m are the composite, fibre and matrix[1] strengths, respectively. However, as with composite moduli, reinforcement is reduced as fibre length is decreased. For mid length fibres ($l > l_c$) the composite strength can be described by

$$\sigma_C = (\eta_s \sigma_f - \sigma_m)V_f + \sigma_m \quad (8)$$

where η_s is the strength efficiency factor, given by $\eta_s = (1 - l_c/2l)$. It should be stressed that when $l > l_c$, the fibres break under large applied stress. However, when $l < l_c$, enough stress cannot be transferred to the fibres to break them and the matrix fails with the fibre pulling out of the matrix.

In this situation, the strength can be described by

$$\sigma_C = (\tau l/D - \sigma_m)V_f + \sigma_m \quad (9)$$

This model describes failure by nanotube pullout, thus the strength is controlled by strength of the matrix–fibre interface, τ, and not the fibre strength. In certain cases the polymer–nanotube interaction may result in the formation of an interfacial polymer region with mechanical properties different to the bulk polymer [47]. Under these circumstances failure may occur at the bulk polymer-interfacial polymer interface. The composite strength is then given by

$$\sigma_C = (1 + 2b/D)[\sigma_{Shear} l/D - (1 + 2b/D)\sigma_m]V_f + \sigma_m \quad (10)$$

where b is the thickness of the interfacial region and σ_{Shear} is the shear strength of the interface [48].

Another common model is that developed by Halpin and Tsai [49]. This was originally developed for continuous fibre composites and follows on from the work of Hill [50].

[1] In Eqs. (7)–(9), it is more correct to replace σ_m with the stress in the matrix when the sample fails. However this can be approximated by σ_m with reasonable accuracy.

For aligned fibre composites, the Halpin–Tsai model gives the composite modulus to be

$$Y_C = Y_m \frac{(1+\zeta\eta V_f)}{(1-\eta V_f)} \tag{11}$$

where $\zeta = 2l/D$ and

$$\eta = \frac{Y_f/Y_m - 1}{Y_f/Y_m + 1} \tag{12}$$

For randomly orientated composites the expression gets slightly more complicated:

$$\frac{Y_C}{Y_m} = \frac{3}{8}\left[\frac{1+\zeta\eta_L V_f}{1-\eta_L V_f}\right] + \frac{5}{8}\left[\frac{1+2\eta_T V_f}{1-\eta_T V_f}\right] \tag{13}$$

where

$$\eta_L = \frac{Y_f/Y_m - 1}{Y_f/Y_m + \zeta} \tag{14}$$

and

$$\eta_T = \frac{Y_f/Y_m - 1}{Y_f/Y_m + 2} \tag{15}$$

The Halpin–Tsai equation is known to fit some data very well at low volume fractions but to underestimate stiffness at high volume fraction.

Both models have two factors in common, the stiffness is predicted to scale with both volume fraction and aspect ratio. In both cases a more or less linear increase of modulus with volume fraction is predicted. This suggests that a good measure of the reinforcement is given by dY_C/dV_f at low V_f. This takes into account both the magnitude of the stiffness increase and the amount of fibre required to achieve it and has the advantage that it can easily be extracted from experimental data. For the rest of this paper, dY_C/dV_f will be used to represent the magnitude of the reinforcement effect. For brevity we will write this quantity as dY/dV_f and refer to it as the reinforcement. This will be used to allow the comparison of results quoted in the literature.

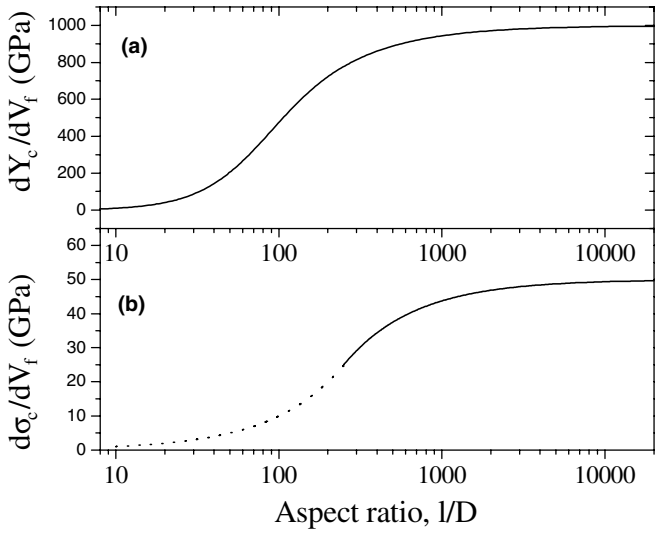

Fig. 3. Modulus reinforcement (a) and strength reinforcement (b) as a function of filler aspect ratio for aligned composites as calculated by the rule of mixtures. Modulus reinforcement is calculated using Eqs. (2), (4) and (5) with $Y_f = 1$ TPa, $Y_m = 1$GPa for a volume fraction of 1%. In part B the strength is calculated for two regimes; $l < l_c$ (dotted line) and $l > l_c$ (solid line) using Eqs. (9) and (8), respectively. The parameters used were $\sigma_f = 50$GPa, $\sigma_m = 10$ MPa and $\tau = 100$ MPa. Using these parameters the critical aspect ratio is $(l/D)_c = 250$. In both A and B these parameters are appropriate for composites of arc discharge MWNT in a polymer matrix with good interfacial shear strength.

In terms of the rule of mixtures (Fig. 3), the reinforcement is then

$$\frac{dY_C}{dV_f} \approx \eta_o \eta_l Y_f - Y_m \tag{16}$$

while for the Halpin–Tsai model (random orientation) the reinforcement is approximated by

$$\frac{dY_C}{dV_f} \approx \frac{3}{8} Y_m \eta_L (\zeta + 1) + \frac{15}{8} Y_m \tag{17}$$

This approximation is valid as $V_f \to 0$ and for stiff fibres where $Y_f \gg Y_m$.

4. System requirements for mechanical reinforcement

There are four main system requirements for effective reinforcement. These are large aspect ratio, good dispersion, alignment and interfacial stress transfer. The effects of aspect ratio have been dealt with in the previous section. Dispersion is probably the most fundamental issue. Nanotubes must be uniformly dispersed to the level of isolated nanotubes individually coated with polymer. This is imperative in order to achieve efficient load transfer to the nanotube network. This also results in a more uniform stress distribution and minimises the presence of stress concentration centres. The effects of poor dispersion can be seen in a number of systems when the nanotube loading level is increased beyond the point where aggregation begins. This is generally accompanied by a decrease in strength and modulus [51].

Alignment is a less crucial issue. As discussed in the previous section, the difference between random orientation and perfect alignment is a factor of five in composite modulus. While alignment is necessary to maximise strength and stiffness, it is not always beneficial. Aligned composites have very an-isotropic mechanical properties, which may need to be avoided in bulk samples. In fibres however alignment has no downside and is a good way to maximise reinforcement.

Probably the most important requirement for a nanotubes reinforced composite is that external stresses applied to the composite as a whole are efficiently transferred to the nanotubes, allowing them to take a disproportionate share of the load. Using the simplistic isostrain approximation where we assume both matrix and nanotubes are equally strained, then the ratio of loads carried by nanotubes to matrix, F_{NT}/F_m is

$$\frac{F_{NT}}{F_m} = \frac{Y_{NT}}{Y_m}\frac{V_f}{(1-V_f)} \quad (18)$$

demonstrating that the fillers take a significantly larger share of the load ($Y_{NT} \gg Y_m$).

In reality, on application of an external stress, σ, the matrix undergoes greater strain, ε, than the nanotube, simply because $Y_{NT} \gg Y_m$ and $\sigma = Y\varepsilon$. This results in a shear stress field, with the shear stress, $\tau_s(r)$, increasing with decreasing distance from the nanotube, r. Adjacent to the nanotube, the shear stress in the matrix, $\tau_s(R)$ can be very large (R is the nanotube radius). It is this matrix shear stress at the interface, $\tau_s(R)$, that controls stress transfer to the nanotube. The force applied to the nanotube, dF, over a length dl is given by [30]

$$dF = 2\pi R\tau_s(R)\,dl \quad (19)$$

In addition it can be shown that $\tau_s(R)$ increases linearly with applied external stress (for small stresses) [30]. This means that the force and hence the stress felt by the nanotube increases linearly with external stress. However at some critical value of the interfacial shear stress, $\tau(R)$, either the matrix in the vicinity of the interface or the matrix–nanotube bond will rupture, resulting in debonding. This value for the shear stress is known as the interfacial shear strength (IFSS) and governs the maximum stress transfer to the nanotube.

The interfacial shear strength is an important parameter for any fibre-reinforced composite and many studies have been devoted to it. The first thing to determine is whether any stress is transferred to the nanotubes at all. It turns out that this is reasonably straightforward to ascertain by Raman spectroscopy. It is well-known that the position of the Raman D' band (located around 2662 cm^{-1}) is sensitive to stress in the nanotubes [52–55]. This peak tends to shift down in frequency when the nanotubes are under tension. The slope of this shift as a function of strain is in principle proportional to the nanotube modulus with a proportionality factor reported to be in the region of -0.2 GPa/cm^{-1} [55].

A body of computational work has been carried out to predict the interfacial shear strength. Frankland et al. used molecular dynamics simulations to estimate the IFSS at ~2.5 MPa for both crystalline and amorphous polyethylene matrices [56]. Liao and Li calculated a much larger value of 160 MPa for PS/NT composites [57] while Wong et al. obtained a similar value of 186 MPa for PS/NT composites and 138 MPa for epoxy/NT composites [58]. In addition Lordi and Yao calculated maximum frictional stresses for a range of polymers coating SWNT [59]. These frictional forces can be associated with the IFSS [60]. Lordi obtained values between 18 and 135 MPa. Wall et al. applied the Frenkel–Kontorova model to ordered monolayers of polymer wrapping SWNT to show that strain induced templating can occur resulting in extremely large stress transfer [61].

While IFSS is challenging to measure for fillers such as nanotubes, some progress has been made. Wagner et al. used observations of stress induced nanotube fracture made in a TEM to estimate a value of 500 MPa [62]. This extremely large value was attributed to covalent bonding between nanotube and matrix. Cooper et al. used an AFM to manipulate nanotubes protruding from holes in an epoxy/NT film. They observed IFSS of 300–400 MPa for tubes with short embedded lengths but values of 30–90 MPa for tubes with longer embedded lengths suggesting that end effects are important [47]. Barber et al. mounted a MWNT onto an AFM tip before pushing it into a heated polymer film. On cooling they measured the force required to pull the tube out, obtaining values between 20 and 90 MPa [63,64] (Fig. 4).

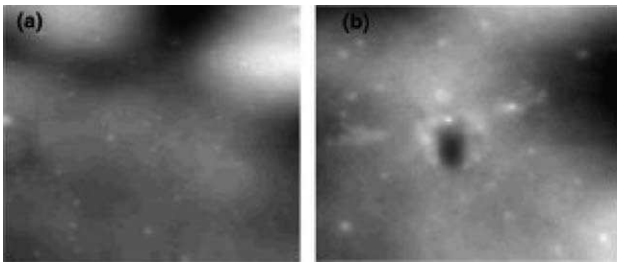

Fig. 4. AFM topography images for polyethylene-butene at room temperature (a) before nanotube insertion and (b) after pullout experiment. The horizontal scan size is 1 μm. Reproduced from [64].

While these values vary significantly, the overlap between experimental and theoretical results seems to suggest that the IFSS lies in the region of 50–100 MPa. However, it should be pointed out that all these results are for non-covalently bonded composites. Much higher values are expected when nanotubes are covalently attached to the matrix [56].

4.1. Polymer–nanotube interactions

Debonding will occur when either the nanotube-matrix interface fails or the matrix fails under the large shear stresses near the interface. In either case it is instructive to consider the interaction between polymer and nanotube in the vicinity of the interface. However, care must be taken here as it is not clear what the relationship should be between the matrix–nanotube binding energy and the IFSS. In fact Lordi and Yao calculated both and found little correlation [59]. It is clear, however that matrix nanotube binding is very dependent on the matrix type [65].

A number of studies suggest that interfacial interactions with nanotubes result in an interfacial region of polymer with morphology and properties different to the bulk. A study from 2002 by McCarthy et al. showed that conjugated polymers can wrap around MWNT [66]. Thicker coatings appeared surprising regular. In addition dendritic polymer growth has been observed to nucleate from defects on the nanotube [66,67]. Coleman and Ferreira showed that polymer wrapping can minimise energy for purely geometric reasons [68]. Computational studies by Wei et al.

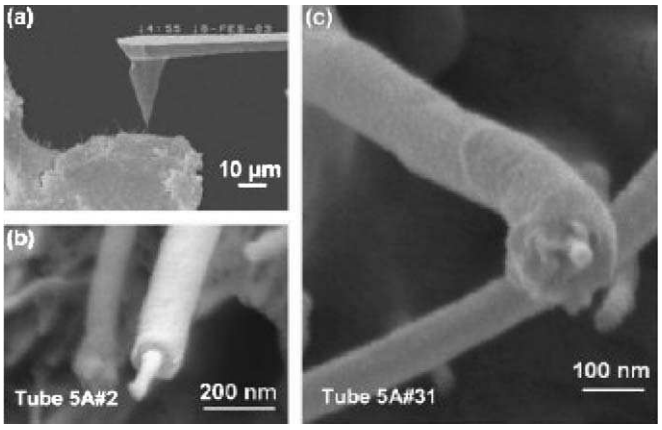

Fig. 5. (a) Far field SEM image of a nanomanipulation experiment inside an SEM. (b, c) High resolution images of polymer coated nanotube structures protruding from a MWNT-polycarbonate fracture surface. Reproduced from [70].

showed that polyethylene adsorbs onto SWNT in ordered monolayers [69].

That these interfacial regions have different properties was shown by Barber et al. In their pullout experiments, the matrix should have fractured before the interface but did not. This suggests that interfacial polymer had anomalously high shear strength [63]. Both Ding et al. [70] (Fig. 5) and Potschke et al. [71] observed thick (10 s of nm) layers of polymer coating nanotubes protruding from composite fracture surfaces. This demonstrates both a high IFSS and a layer of high shear strength polymer. Coleman et al. observed similar behaviour but were able to link it to the formation of a high strength crystalline coating [48]. Assouline et al. observed nucleation of crystallinity in the presence of nanotubes. The crystallites were observed to be fibular in nature as compared to spherical in the pure polymer [72]. Observations of crystallinity nucleation have been made by a number of groups [73–75]. It had previously been shown that the nucleation of transcrystallinity by nanofibres can improve IFSS [76].

While there is much debate as to the nature of the polymer morphology at the interface it is clear that it plays some role in the mechanical reinforcement process. In addition it is very polymer specific. More work is needed to understand this interesting phenomenon.

5. Composite processing

5.1. Solution processing of composites

Perhaps the most common method for preparing polymer nanotube composites has been to mix the nanotubes and polymer in a suitable solvent before evaporating the solvent to form a composite film. One of the benefits of this method is that agitation of the nanotubes powder in a solvent facilitates nanotube de-aggregation and dispersion. Almost all solution processing methods are variations on a general theme which can be summarised as

1. Dispersion of nanotubes in either a solvent or polymer solution by energetic agitation.
2. Mixing of nanotubes and polymer in solution by energetic agitation.
3. Controlled evaporation of solvent leaving a composite film.

In general, agitation is provided by magnetic stirring, shear mixing, reflux or, most commonly, ultrasonication. Sonication can be provided in two forms, mild sonication in a bath or high-power sonication using a tip or horn.

An early example of solution based composite formation is described by Jin et al. [77]. In this work MWNT produced by arc discharge were dispersed in chloroform by sonicating for 1 h. The chosen polymer, polyhydroxyaminoether (PHAE) was then dissolved in the MWNT-chloroform dispersion. Mixing was achieved by applying another hour of sonication. The suspension was then poured into a Teflon mould and dried in ambient conditions overnight in a fume-hood. By this method, high loading levels of up to 50 wt.% and reasonably good dispersions were achieved.

In most subsequent studies, a slight variation was used. Shaffer and Windle [78] dispersed chemically modified catalytic MWNT in water. This was carefully blended with solutions of polyvinylalcohol in water to give composite dispersions which could be drop cast to form films with up to 60 wt.% nanotubes. Qian et al. [79] used sonication to disperse catalytic MWNT in toluene. This was then blended with a solution of polystyrene, also in toluene. Mixing was achieved by further sonication before drop casting to form films. This technique has been used subsequently by many groups [80,81]. Ruan et al. [54] followed a similar method but used magnetic stirring and sonication to disperse the nanotubes but reflux to mix the nanotubes and polymer.

It should be pointed out that this method relies on the efficient dispersion of nanotubes in the relevant solvent. The choice of solvent is generally made based on the solubility of the polymer. However pristine nanotubes cannot be well-dispersed in most solvents. To get around this problem a number of groups have used an additive such as a surfactant to disperse the nanotubes before mixing with the polymer solution [82–84]. The most common choices of surfactant are derivatives of sodium dodecylsulfate (SDS). This technique results in excellent dispersion with no derogatory effects on film properties observed. In a similar technique the pH of the dispersion is controlled by addition of HCl again resulting in good dispersion and wetting [85].

A number of papers have discussed dispersion of nanotubes in polymer solutions [48,86]. This can result in good dispersion even when the nanotubes cannot be dispersed in the neat solvent. Coleman et al. used sonication to disperse catalytic MWNT in polyvinylalcohol/H_2O solutions, resulting in a MWNT dispersion that was stable indefinitely. Films could be easily formed by drop-casting with

microscopy studies showing very good dispersion. Cadek et al. showed that this procedure could also be applied to arc discharge MWNT, double wall nanotubes (DWNT) and Hipco SWNT. In a separate paper [87] also showed that this procedure could be used to purify arc-MWNT by selective sedimentation during composite production.

5.2. Melt processing of bulk composites

While solution processing is a valuable technique for both nanotube dispersion and composite formation, it is completely unsuitable for the many polymer types that are insoluble. Melt processing is a common alternative, which is particularly useful for dealing with thermoplastic polymers. This range of techniques makes use of the fact that thermoplastic polymers soften when heated. Amorphous polymers can be processed above their glass transition temperature while semi-crystalline polymers need to be heated above their melt temperature to induce sufficient softening. Advantages of this technique are its speed and simplicity, not to mention its compatibility with standard industrial techniques [88,89].

In general, melt processing involves the melting of polymer pellets to form a viscous liquid. Any additives, such as carbon nanotubes can be mixed into the melt by shear mixing. Bulk samples can then be fabricated by techniques such as compression molding, injection molding or extrusion. However it is important that processing conditions are optimised, not just for different nanotube types, but for the whole range of polymer–nanotube combinations. This is because nanotubes can effect melt properties such as viscosity, resulting in unexpected polymer degradation under conditions of high shear rates [90].

An early study on the melt mixing of arc discharge MWNT and polymer was carried out by Jin et al. [91] in 2001. They mixed polymethylmethacrylate (PMMA) with 26 wt.% MWNT in a laboratory mixing moulder at 200 °C. The melt was then compression moulded (under 8–9 MPa at 210 °C) in a hydraulic press to give composite slabs. TEM studies showed that dispersion was good even at high MWNT concentration.

In two papers in 2002 Andrews and co-workers showed that commercial polymers such as high impact polystyrene, polypropylene and acrylonitrile–butadiene–styrene (ABS) could be melt processed with CVD-MWNT to form composites [92]. The polymers were blended with nanotubes at high loading level in a high shear mixer to form masterbatches. These masterbatches were then mixed with pure polymer to form lower mass fraction samples. Films were formed by compression molding. Studies of the nanotube dispersion during mixing showed a significant improvement as the total mixing energy was increased. This can be achieved either by increasing the residence time or mixing speed. However it was found that the average nanotube length fell with mixing energy. For the samples with the best dispersion, the nanotube length had fallen to a quarter of its initial value. A similar combination of shear mixing and compression molding was also used by a number of other groups [51,93,94].

Potschke et al. blended masterbatches of CVD-MWNT in polycarbonate with pure polycarbonate in a microcompounder at 260 °C [90]. Test samples were then fabricated by extruding through a circular die. It was found that a small-scale extruder was just as efficient as a larger scale model. However, some polymer degradation was observed in the composites due to the higher shear rates need to overcome the increased viscosity due to the presence of the nanotubes. Extrusion was also used by Gorga and Cohen [95]. They dry blended PMMA with both Carbolex SWNT and CVD-MWNT before using a twin screw extruder at 130 °C to extrude the sample through a cylindrical die. The nanotubes were successfully aligned by melt drawing the extruded rods.

Injection molding has also been used to fabricate composites. Meincke et al. mixed polyamide-6, ABS and CVD-MWNT in a twin screw extruder at 260 °C [96]. The extrudate was broken up into pellets and injection molded to form test samples. Very good nanotube dispersions were observed by TEM. Another example of using combined techniques was demonstrated by Tang et al. [97]. High density polyethylene pellets and nanotubes were melted in a beaker, then mixed and compressed. The resulting solid was broken up and added to a twin screw extruder at 170 °C and extruded through a slit die. The resulting film was then compression molded to form a thin film.

In some cases shear mixing can be difficult as the nanotube powder tends to stick to the walls of the mixer. To overcome this, a combination of solution and melt techniques can be used. Thostenson and Chou initially dispersed CVD-MWNT in a solution of PS in tetrahydrofurane (THF) [98]. This was then drop cast and dried to form a film. This film was cut up and extruded through a rectangular die. Films could be formed by compression molding or alternatively the nanotubes could be aligned by drawing the sample direct from the extruder. In both cases very good adhesion and wetting were observed. Cooper et al. mixed PMMA microspheres and SWNT in ethanol [99]. While this did not dissolve the PMMA, it resulted in a coating of immobilized nanotubes on each sphere. The sample was dried and then ball milled before mixing in a twin screw compounder. Films were extruded through a slit die with significant nanotubes alignment observed.

5.3. Melt processing of composite fibres

For many applications fibres are more suitable than bulk materials. In addition, fibres production techniques tend to be suited to the alignment of nanotubes within the fibre. A number of studies have focused on production of composite fibres by melt processing.

One of the earliest studies on melt processing of polymer–nanotubes composites was carried out by Haggenmueller et al. [100] (Fig. 6). They demonstrated the production of composite fibres through a rather complicated process.

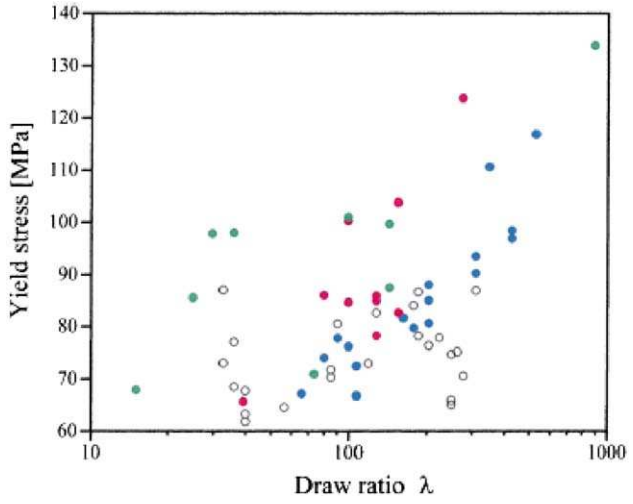

Fig. 6. Yield stress versus draw ratio for SWNT-PMMA melt spun fibres. Reproduced from [100].

SWNT and PMMA were dispersed dimethylformamide (DMF), blended and dried. The resultant films were broken up and hot pressed to form a new film. This was then broken up and hot pressed, a process that was repeated as many as twenty five times. The resulting composite film was then extruded through a 0.6 mm cylindrical die and drawn under tension to form a fibre. The authors observed that the nanotubes dispersion improved with each melting step. After a large number of such steps the composite consisted of very well-dispersed, highly aligned nanotubes.

In the study by Andrews et al. described above, fibres were also produced [92]. The composite was extruded through a 0.3 mm diameter die and then rapidly drawn to a final diameter of 20–75 μm. Two studies from the Oklahoma group demonstrated fibre spinning from PP and SWNT using a ram extruder through a 1.27 mm die [101,102]. Fibres were drawn at high speed onto take up roll resulting in final diameters of 50–60 μm. The alignment was improved even further by post-drawing at elevated temperature.

Sandler et al. compared fibres made from polyamide-12 with a range of fillers: arc-MWNT, vapor grown carbon fibres (VGCF) and both aligned and entangled CVD-MWNT [103]. Polymer pellets and NT powder were mixed in a twin screw microextruder. The extrudate was chopped and fed into a capillary rheometer with 1 mm die. Fibres were spun at 0.5 m/s to produce a final fibre diameter of 125 μm. The observed dispersion and alignment was very good for the CVD-MWNT. However the arc-MWNTs were less well-dispersed. In addition voids were seen in the fibres fabricated from arc-MWNT (Fig. 7).

Finally, Chang et al. used solution dispersion to mix SWNT with PP. fibres were spun using an Instron capillary rheometer with a die diameter of 1.6 mm followed by fibre collection on a high speed take up roll. Polarised Raman studies were carried out to assess the degree of alignment.

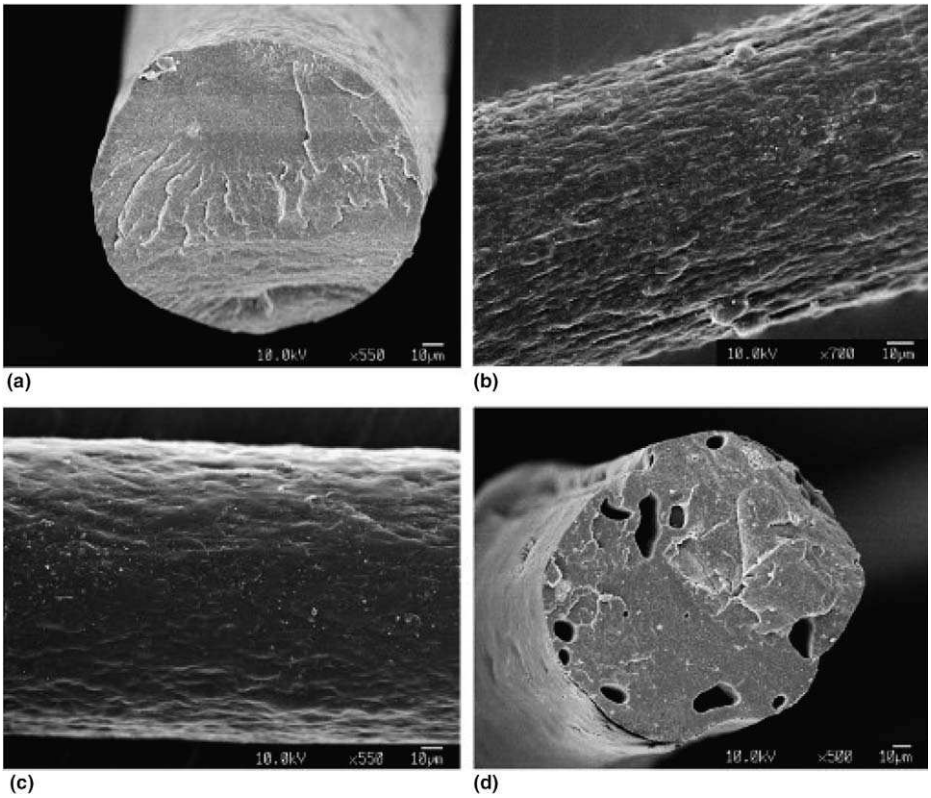

Fig. 7. SEM images of composite fibres containing (a) carbon nanofibres, (b) entangled MWNT, (c) aligned MWNT and (d) arc-MWNT. Reproduced from [103].

A polarised Raman ratio ($=/\perp$) of ~5 was observed with no dependence on nanotube mass fraction or draw ratio.

5.4. Processing of composites based on thermosets

The most common thermosetting polymers used in the formation of polymer nanotube composites have been epoxy resins. Generally these are polymers that cure when mixed with a catalyzing agent or hardener. In most cases the epoxy begins life in liquid form, facilitating nanotube dispersion by the techniques described in Section 5.1. Curing is then carried out to convert the liquid composite to the final solid state.

In the simplest cases nanotubes have been dispersed by sonication in a liquid epoxy such as Shell EPON 828 epoxy [52]. This blend is then cured by the addition of hardener such as triethylene tetramine in the case of Ref. [52]. After having been left to gel overnight the composite was cured at 100 °C for 2 h.

While this is the simplest case, a number of variations have been described. Li et al. improved the initial nanotube dispersion by dispersing the nanotubes in a solution of a block co-polymer (Disperbyk-2150) in ethanol [104]. A liquid epoxy was then added and the ethanol removed by evaporation. The hardener was added and the composite poured into a mould and cured in a vacuum oven at 25 °C for 18 h.

In a similar vein, Lau et al. initially dispersed nanotubes in DMF, ethanol and acetone by sonication before adding the epoxy [105]. After further sonication the solvents were removed by evaporation. The mixture was then cast in a mould and the hardener added. Curing was carried out on a hotplate at 50 °C for 10 min followed by 24 h at room temperature. They found that while dispersion was improved, traces of residual solvents had a negative effect on the composite properties.

In a slightly different technique, Xu et al. dispersed nanotubes in chloroform before adding a photoresist epoxy [106]. In this case no hardener was needed. Films were formed by spin coating before curing by baking followed by exposure to UV light.

Finally composites have been fabricated from amide-oligomer based thermosets [107]. The nanotubes and the oligomer material were first dry mixed in a mechanical blender. The mixture was then melted in a hotpress at 320 C° before curing at 370 °C under a pressure of 0.2 MPa for an hour.

5.5. Novel composites

A number of novel composite preparation methods have been described that are distinct from the traditional methods described above. While some of these methods such as electrospinning and coagulation spinning have been used industrially for years, we have included them in this section as they are not commonly used in the field of polymer–nanotube composites.

5.5.1. Composite films

The simplest of these methods involves the infiltration of polymer from solution into pre-existing nanotube networks. This concept was first demonstrated by Coleman et al. [108] in 2003. They first made thin sheets of SWNT by Buchner filtration (Buckypaper). This paper is extremely porous and contains up to 70% free volume. These sheets were then soaked in polymer solutions for various times before rinsing. Microscopy images of fracture surfaces showed that the polymer had intercalated throughout the paper. In this way polymer mass fractions of up to 30 wt.% could be incorporated (Fig. 8).

A similar technique was demonstrated by Wang et al. [109]. They also fabricated Buckypaper but incorporated an epoxy-hardener blend by Buchner filtration. To reduce the viscosity the blend was mixed with ethanol. Very good infiltration was observed throughout the paper. The epoxy was cured by hotpressing 3–5 stacked sheets together at 177 °C to form a thick composite film.

An alternative method involves the growth of nanotube forests on patterned substrates by CVD [110]. A polymer polydimethylsiloxane (PDMS) could then be spincoated on top of the forest. The polymer infiltrates the forest during spin coating. In this work the polymer was cured after infiltration at room temperature for 24 h. The composite film can then easily be peeled from the substrate. The advantage of this method is that the geometry of the nanotubes network can be predetermined by the growth conditions in the CVD chamber.

Another interesting method, first described by Mamedov [111] and subsequently refined by others [112,113] is the layer by layer (LBL) assembly method. This involves building up a layered composite film by alternate dipping of a substrate into dispersions of SWNT and polyelectrolyte solutions. In this way as many as 40 layers are built up. In order to further enhance the structural integrity of the film, cross-linking can be induced. After every fifth deposition cycle, a layer of MWNTs was replaced with a layer of polyacrylamide (PAA) to introduce carboxyl functionalities for amide cross-linking between polyelectrolytes. The film was then heated to 120 °C for 30 min, resulting in amide bonds between PAA and polyethylisophthalate (PEI). In addition, covalent bonds also form between PEI and MWNT at these temperatures. This method has significant advantages. Film properties such as thickness and polymer–nanotube ratio can be controlled easily. In addition very high nanotube loading levels can be obtained.

5.5.2. Composite fibres

Composite fibres can be produced by solution based methods as well as the traditional melt spinning method. An elegant method was demonstrated by Vigolo et al. in 2000 [114]. In this work SWNT were dispersed in water with the aid of a surfactant. This dispersion was then injected into a rotating bath of polyvinylalcohol dissolved in water such that nanotube and PVA dispersions flowed in the same direction at the point of injection. Polymer

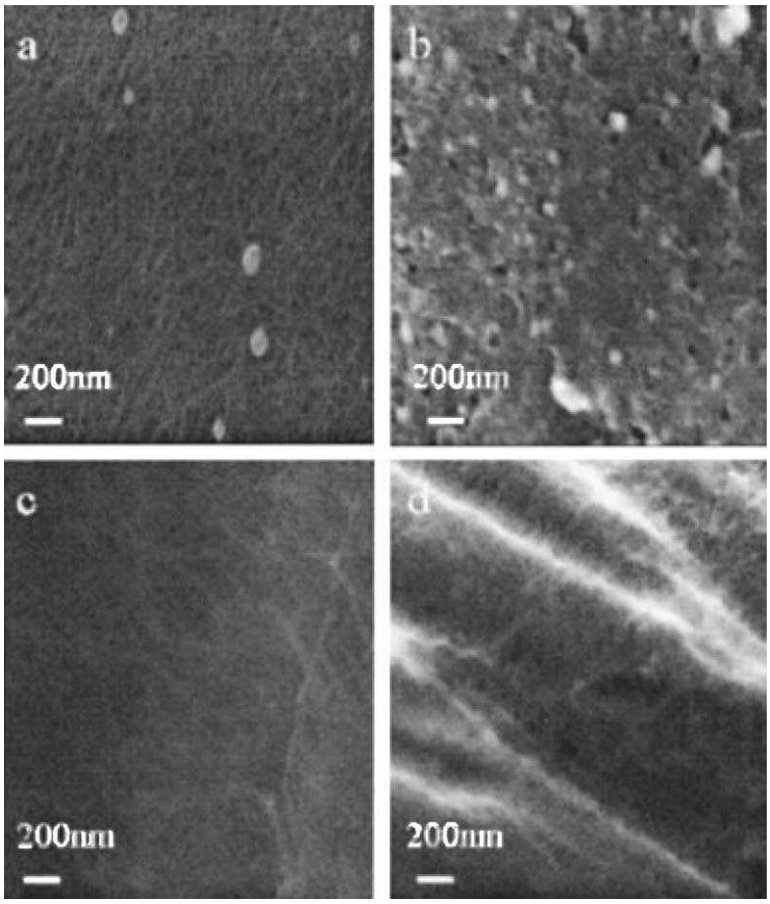

Fig. 8. Scanning electron micrograph images of typical reference (pristine) and polymer soaked Buckypaper. (a) Surface and (c) cross-section of reference paper. (b) Surface and (d) cross-section of paper soaked in a polymer solution. Reproduced from [108].

molecules then tend to replace surfactant molecules on the nanotube surface thus de-stabilizing the nanotubes dispersion which collapses to form a fibre. These wet fibres can then be retrieved from the bath, rinsed and dried. Significant rinsing is used to remove both surfactant and PVA. Shear forces during the flow lead to nanotube alignment. However, the fibres can be re-wetted and dried under tension. This results in significantly enhanced alignment.

This method was further improved by Dalton et al. [115]. They injected the nanotubes dispersion into the centre of a co-flowing PVA/water stream in a closed pipe. The wet fibre was then allowed to flow through the pipe for approximately a meter before being wound on a rotating mandrel. Flow in more controllable and more uniform conditions in the pipe resulted in longer (~100 m) and more stable fibres. Crucially, wet fibres were not rinsed to remove PVA although they were dried to produce fibres with final diameters of tens of microns. Furthermore, Miaudet et al. [116] have shown that these fibres can be drawn at temperatures above the PVA glass transition temperature, resulting in improved nanotube alignment and polymer crystallinity.

Another method used recently to form composite based fibres from solution is electrospinning. This technique has been used to produce man-made fibres since 1934 [117] and involves electrostatically driving a jet of polymer solution out of a nozzle onto a metallic counter-electrode. In a paper in Advanced Materials in 2003 Ko et al. described electrospinning as a method to fabricate polymer–nanotube composite fibres and yarns [118]. Composite dispersions of SWNT and either polylactic acid (PLA) or polyacrylonitrile (PAN) in DMF were initially produced. The dispersion was then placed in a pipette with a 0.9 mm nozzle. A wire was placed in the pipette and connected to a steel plate, via a high voltage power supply (25 kV). The plate was 15 cm below the nozzle. When the power supply is turned on, the composite solution becomes charged. This forces it out of the nozzle and towards the counter electrode. Charging of the solvent causes rapid evaporation resulting in the coalescence of the composite into a fibre which can be collected from the steel plate. Fibres with diameters between 10 nm and 1 μm can be produced in this fashion. In Ko's paper, dispersion of the nanotubes within the fibres was polymer dependent with much better dispersion and alignment observed in the PAN fibres. Yarns were also produced by collecting the fibres on a rotating drum and twisting them.

In a similar study, Sen et al. formed fibre based membranes [119]. They spun from SWNT dispersed in either polystyrene or polyurethane with a 3 cm needle-plate gap.

In this work the solution was pumped slowly out of a needle under the application of 15 kV. Spinning was continued for 1 h until the counter-electrode was covered in a membrane built up from the spun fibres. For the PS based dispersions these membranes were clearly fibrous. However, for the PU based fibres the membranes were wet looking and ribbon-like suggesting incomplete solvent evaporation.

5.6. In situ polymerisation processing

Over the last 5 years in situ polymerisation in the presence of carbon nanotubes has been intensively explored for the preparation of polymer grafted nanotubes and processing of corresponding polymer composite materials. The main advantage of this method is that it enables grafting of polymer macromolecules onto the walls of carbon nanotubes. In addition, it is a very convenient processing technique, which allows the preparation of composites with high nanotube loading and very good miscibility with almost any polymer type. This technique is particularly important for the preparation of insoluble and thermally unstable polymers, which cannot be processed by solution or melt processing. Depending on required molecular weight and molecular weight distribution of polymers, chain transfer, radical, anionic, and ring-opening metathesis polymerizations can be used for in situ polymerization processing. Here we consider only recent advances in situ polymerization processing, which resulted in new polymer–carbon nanotube composites with improved mechanical properties.

Initially, in situ radical polymerization was applied for the synthesis of poly(methyl methacrylate) (PMMA)–MWNT composites by Jia et al. [120]. In this work, in situ polymerization was performed using radical initiator 2,2′-azobisisobutyronitrile (AIBN). The authors believed that π-bonds in carbon nanotubes were initiated by AIBN and therefore nanotubes could participate in PMMA polymerization to form a strong interface between the MWNTs and the PMMA matrix. Velasco-Santos et al. have also used AIBN as initiator of in situ radical polymerization to incorporate both unfunctionalised and carboxyl functionalised MWNTs into a PMMA matrix [121]. Then, more recently, Putz et al. reported preparation of SWNT–PMMA composites via the dispersion of SWNTs in a monomer solution followed by in situ radical polymerization initiated again by AIBN [122].

Kumar et al. have synthesised new ultra-strong poly(*p*-phenylene benzobisoxazole) (PBO) composites in the presence of single-wall carbon nanotubes (SWNTs) in poly(phosphoric acid) (PPA) by in situ PBO polymerization [123]. After the polymerization PBO/SWNT composite fibres have been spun from the liquid crystalline solutions using dry-jet spinning.

In situ polymerisation was also very useful for the preparation of polyamide–carbon nanotube polymer composites. For instance, polyamide 6 (PA6)/MWNTs composites have been prepared by in situ hydrolytic polymerization of ε-caprolactam in the presence of pristine and carboxylated nanotubes [124]. ε-Caprolactam monomer was found to form an electron-transfer complex with MWNTs giving a homogeneous polymerizable master solution, which facilitates the formation of composites with homogenously dispersed nanotubes. In other work, Gao et al. reported new improved chemical processing technology that allows the continuous spinning of SWNT–nylon 6 (PA6) fibres by the in situ ring opening polymerization of caprolactam in the presence of SWNT [125]. This process results in a new hybrid material with characteristics of both the fibre and the matrix, with an excellent compatibility between the SWNTs and nylon 6.

Park et al. also reported the synthesis of SWNT reinforced polyimide composites by in situ polymerization of diamine and dianhydride under sonication [126].

The in situ epoxidation reaction has also been used for the preparation and processing of epoxy based polymer composites. For instance, carboxyl and fluorine functionalised SWNTs have been integrated into epoxy polymer via formation of covalent bonds by in situ epoxy ring-opening esterification and amine curing chemical reactions [127]. The same group has further developed fully integrated nanotube epoxy composite material with direct covalent bonding between the matrix and SWNTs using functionalised SWNTs prepared via diamine reactions with alkyl–carboxyl groups directly attached to the SWNTs sidewalls [128]. Khabashesku and co-workers has also demonstrated that the fluorination of SWNTs and subsequent reactions with terminal diamines results in the sidewall amino-functionalised nanotube precursors for the preparation of nylon-SWNT polymer composites [129]. Another group reported preparation and investigation of composites based on epoxy resin and different weight percentage of amino-functionalised and non-functionalised MWNTs [130].

In general, in situ polymerization can be applied for the preparation of almost any polymer composites containing carbon nanotubes which can be non-covalently or covalently bound to polymer matrix. Non-covalent binding between polymer and nanotube involves physical adsorption and wrapping of polymer molecules through van der Waals and π–π interactions. The role of covalently functionalised and polymer grafted nanotubes will be considered in more detail below.

5.7. Covalent functionalisation and polymer grafting of nanotubes

Covalent functionalisation and surface chemistry of single-walled carbon nanotubes have been envisaged as very important factors for nanotube processing and applications [131]. Due to the relatively smooth graphene like surface of nanotubes, there is a lack of interfacial bonding between polymer matrix and carbon nanotubes. Nanotubes, in particular SWNTs, are typically held together as bundles resulting in poor nanotube dispersion in polymer matrices. Chemical functionalisation of the nanotube surface is

expected to resolve these problems. However, it was shown that covalent chemical attachments may decrease the maximum buckling force of nanotubes by about 15% and therefore reduce the mechanical properties of the final nanotube composite [132]. Recently, many efforts on polymer composites reinforcement have been focused on an integration of chemically modified nanotubes containing different functional groups into the polymer matrix. Covalent functionalisation can be realised by either modification of surface-bound carboxylic acid groups on the nanotubes or direct addition of reagents to the sidewalls of nanotubes. As discussed previously, in situ polymerization is also one of the main approaches for the preparation of polymer grafted nanotubes. Therefore work on the preparation of polymer grafted nanotubes frequently overlaps with in situ polymerization processing. Here we are going to discuss only recent advances in the production of functionalised and polymer grafted of nanotubes, which have been used to improve mechanical properties of polymer composites.

Two main strategies for the covalent grafting of polymers to the nanotubes have been reported: "grafting from" and "grafting to". The "grafting from" method is based on the initial immobilization of initiators onto the nanotube surface followed by the in situ polymerization of appropriate monomers with the formation of the polymer molecules bound to the nanotube. The advantage of this technique is that polymer–nanotube composites with quite high grafting density can be prepared. However, this method requires a strict control of amounts of initiator and substrate as well as a control of conditions for polymerization reaction. The "grafting to" approach is based on attachment of already preformed end-functionalised polymer molecules to functional groups on the nanotube surface via different chemical reactions. An advantage of this method is that preformed commercial polymers of controlled mass and distribution can be used. The main limitation of the "grafting to" technique is that initial binding of polymer chains sterically prevents diffusion of additional macromolecules to the surface leading to low grafting density. Also only polymers containing reactive functional groups can be used.

An example of the "grafting from" strategy is a treatment of SWNTs with *sec*-butyllithium that generates carbanions on the nanotube surface. These carbanions serve as initiators of anionic polymerization of styrene for in situ preparation of polystyrene-grafted nanotubes [133]. This procedure allows the debundling of SWNTs and produces homogeneous dispersion of nanotubes in polystyrene solution.

The "grafting from" technique is widely used for the preparation of PMMA and related polymer grafted nanotubes. For example, Qin et al. reported the preparation of poly(*n*-butyl methacrylate) grafted SWNTs by attaching *n*-butyl methacrylate (*n*BMA) to the ends and sidewalls of SWNT via atom transfer radical polymerization (ATRP) using methyl 2-bromopropionate as the free radical initiator [134]. A similar approach was reported by Hwang et al. for synthesis of PMMA grafted MWNTs by potassium persulfate initiated emulsion polymerization reactions and use of the grafted nanotubes as a reinforcement for commercial PMMA by solution casting [135]. Xia et al. used an ultrasonically initiated in situ emulsion polymerization to functionalise MWNTs with poly(butylacrylate) (PBA) and PMMA polymers. Then these polymer-encapsulated carbon nanotubes could be used to reinforce a Nylon 6 matrix [136].

Using the "grafting from" approach Tong et al. have modified SWNTs with polyethylene (PE) by in situ Ziegler–Natta polymerization. In this work the surface of the SWNTs was initially functionalised with the catalyst ($MgCl_2/TiCl_4$), and then the ethylene was polymerized thereby giving PE grafted SWNTs, which were mixed with commercial PE by melt blending [137].

One of the first examples of the "grafting to" approach was published by Fu et al. in 2001 [138]. In this work carboxylic acid groups on the nanotube surface were converted to acyl chlorides by refluxing the samples in thionyl chloride. Then the acyl chloride functionalised carbon nanotubes were reacted with hydroxyl groups of dendritic PEG polymers via the esterification reactions.

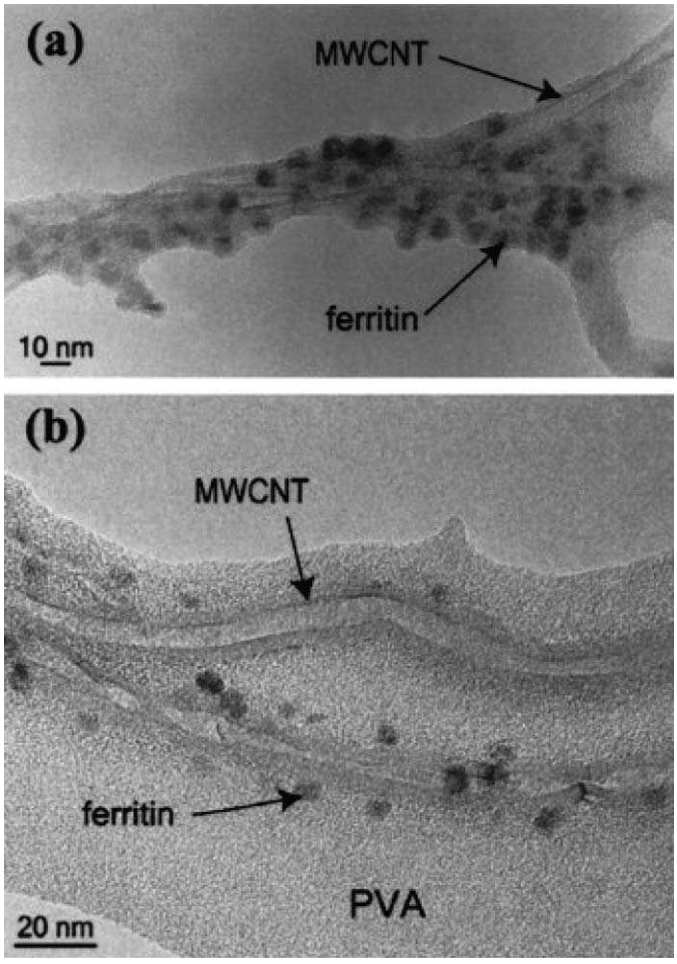

Fig. 9. TEM images of MWNT with attached ferratin molecules. Reproduced from [140].

Another original example of the "grafting to" approach have been reported by Lou et al. [139]. In this work MWNTs have been grafted to polystyrene, poly(ε-caprolactone), and their block copolymers by addition reaction of the corresponding alkoxyamine-terminated precursors.

The "grafting to" method was used for the preparation of composites with the polymers containing reactive functional groups. For example, Bhattacharyya et al. have developed new fully integrated nanotube–PVA composite materials through the functionalisation of MWNTs by covalently attaching ferritin protein molecules onto the surface of nanotubes [140] (Fig. 9). Liu et al. also reported the preparation of poly(vinyl alcohol) (PVA) composites with hydroxyl functionalised SWNTs by simple mixing [141].

A new organometallic modification of the "grafting to" strategy was recently introduced by Blake et al. [142]. In this work MWNTs have been initially organometallically functionalised using *n*-butyllithium and then covalently bonded to a chlorinated polypropylene (CPP) via a coupling reaction with an elimination of LiCl. The addition of the CPP-grafted nanotubes to the CPP polymer matrix resulted in significant increase of mechanical properties.

In addition to the "grafting from" and "grafting to" strategies, there are also a few other techniques to incorporate functionalised carbon nanotubes into polymer matrix. For instance, using the amidisation reaction of octadecylamine with nanotubes, Yang et al. prepared functionalised soluble MWNTs and mixed them in solution with a methyl and ethyl methacrylate (P(MMA-co-EMA)) co-polymer at various loadings [143]. Broza et al. prepared new poly(butylene terephthalate) (PBT)–nanotube composites by introducing the oxidized SWNTs into the reaction mixture during two-stage polycondensation of buthylene terephthalate in molten state. After polycondensation the composites were extruded followed by injection molding [144].

In partial summary, covalent functionalisation and polymer grafting of carbon nanotubes can provide an efficient homogeneous dispersion of nanotubes in the polymer matrix and excellent interfacial stress transfer between a nanotube and polymer.

6. Mechanical properties of polymer nanotube composites

In this section we will discuss results from the literature on mechanical properties of polymer nanotube composites. Many studies have been published each with a different focus. However, the common theme seems to have been enhancement of Young's modulus. In order to attempt to compare different studies we will use the Young's modulus reinforcement, dY/dV_f, as a yardstick. In most papers this quantity is not quoted so we have attempted to evaluate it from the data presented. As this procedure potentially results in a large error, this quantity is to be taken as a guide only.

6.1. Mechanical properties of solution processed composites based on thermoplastic polymers

In this section mechanical properties of solution based composites will be presented. All results pertaining to Young's Moduli are summarised in Table 1.

The first study using nanotubes for reinforcement of solution based composites was by Shaffer and Windle [78] in 1999. They carried out DMTA measurements on CVD-MWNT-PVA films with nanotube weight fractions of up to 60%. Very little reinforcement was observed, with the storage modulus increasing from approximately 6 GPa for the polymer to 12 GPa for the 60 wt.% composite film. While better results were observed above the polymer glass transition temperature, this is a reflection of the fact that it is easier to reinforce softer matrices. Analysis using short fibre theory gave a value for nanotube modulus and effective length of 150 MPa and 35 nm, respectively. The low modulus value may be reflective of the difficulty in fitting a highly non-linear function such as Krenchel's rule of mixtures to a limited data set. In any case this work showed

Table 1
Moduli of solution based matrices and their composites

Nanotube type	Polymer	Y_{Poly} (GPa)	Y_{Max} (GPa)	Max NT content	dY/dV_f (GPa)	Comment	Reference and year
CVD-MWNT	PVA	~6.3	~12.6	60 wt.%	~4.7	DMA	[78] 1999
CVD-MWNT	PS	1.2	1.69	1 wt.%	~74	TT	[79] 2000
Arc-MWNT	PVA	7	12.6	0.6 vol.%	990	NHT. Probably too big by ~×3.5	[87] 2002
Arc-MWNT	PVK	2	5.6	4.8 vol.%	75	NHT	[87] 2002
CVD-MWNT	PSBA (elastomer)	0.52×10^{-3}	3.54×10^{-3}	8.3 vol.%	35×10^{-3}	TT	[82] 2002
CVD-MWNT	PS	1.53	3.4	2.5 vol.%	122	TT	[80] 2002
CVD-MWNT	HDPE	0.98	1.35	1 wt.%	57	TT	[54] 2003
Arc-MWNT	MEMA	0.71	2.34	1 wt.%	272	DMA	[81] 2003
DWNT	PVA	2	3.6	0.2 vol.%	1244	TT	[86] 2004
CVD-MWNT			4.2	0.6 vol.%	376		[86] 2004
CVD-MWNT			3.2	0.6 vol.%	240		[86] 2004
CVD-MWNT			3.0	0.6 vol.%	204		[86] 2004
Arc-MWNT			3.6	1.5 vol.%	128		[86] 2004
SWNT			3.2	2 vol.%	112		[86] 2004
CVD-MWNT	PVA	1.9	7.04	0.6 vol.%	754	TT	[48] 2004

The abbreviations DMA, TT and NHT refer to dynamic mechanical analysis, tensile testing and nanohardness testing, respectively.

that while reinforcement was possible, much work was still needed.

Shortly afterwards Qian et al. [79] studied CVD-MWNT-PS composites using tensile testing. They observed an increase in modulus from 1.2 GPa for PS to 1.62 GPa and 1.69 GPa for composites filled with 1 wt.% short (~15 μm) and long (~50 μm) tubes, respectively. These increases are equivalent to reinforcement values of $dY/dV_f \sim 64$ GPa and $dY/dV_f \sim 74$ GPa. In addition, the tensile strength increased from 12.8 MPa for the polymer to 16 MPa for both tube types at 1 wt.% loading.

In an attempt to understand the reinforcement mechanism, Qian et al. initiated crack formation inside a TEM. They were then able to observe the appearance of crazes where cracks were bridged by nanotubes. When the crazes reached widths of ~800 nm, the nanotubes were seen to either fracture or pull out of the matrix. This suggests that the interfacial bonding is not totally uniform with some weak spots facilitating pullout. In addition, it shows that nanotubes are limited mechanically by their weakest points which are most probably associated with structural defects (Fig. 10).

Safadi et al. [80] also studied composites made from CVD-MWNT and PS by tensile testing. They found an increase in modulus from 1.53 GPa for the polymer to 3.4 GPa for a 2.5 vol.% composite ($dY/dV_f = 122$ GPa) and a strength increase from 19.5 MPa to 30.6 MPa at the same loading level. Interestingly enough, similar increases were observed for both dropcast thick films (400 μm) and spin cast thin films (40 μm) indicating that nanotube orientation varies little with film thickness in that range. In addition both tube fracture and pullout were observed in agreement with Qian's work. However it should be pointed out that another microscopy study on fracture surfaces using arc-MWNT based composites observed pullout but no nanotube breakage [85]. This underlines the problems associated with the low strength of CVD nanotubes.

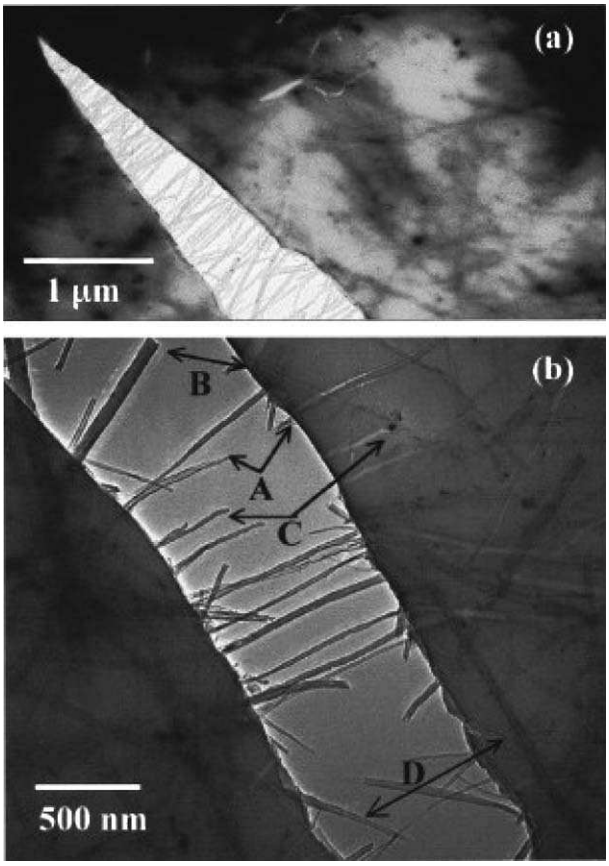

Fig. 10. In situ observation of crack nucleation and propagation in MWNT-PS thin films as induced by thermal stresses. Reproduced from [79].

Polyvinylalcohol was revisited as a matrix material by Cadek et al. [87] in 2002. They carried out nanohardness tests on spun cast films of arc-discharge MWNT in both PVA and polyvinylcarbazole (PVK). Increases in modulus from 7 GPa to 12.6 GPa with 0.6 vol.% MWNT in PVA and from 2 GPa to 5.6 GPa with 4.8 vol.% in PVK were observed. These increases are equivalent to reinforcement values of $dY/dV_f = 990$ GPa and $dY/dV_f = 75$ GPa for PVA and PVK, respectively. However the value for PVA is probably artificially inflated as modulus values for PVA are known to be closer to 2 GPa [5]. This suggests that the reinforcement value for PVA should be scaled down to $dY/dV_f \sim 280$ GPa. Crucially Cadek et al. studied the morphology of the polymer matrices using differential scanning calorimetry (DSC). They observed the PVA crystallinity increasing linearly with nanotube content. This suggests the nucleation of crystallinity by the nanotubes. No such effect was observed for the PVK samples. This suggests that the difference in reinforcement may be related to the presence of a crystalline interface for PVA composites but an amorphous one for PVK materials. This indicates the possibility that stress transfer may be maximised by the presence of an ordered interface as suggested by Frankland et al. [56].

However, Velasco-Santos et al. measured reasonably large increases in modulus from 0.71 GPa for a methyl-ethyl-methacrylate co-polymer to 2.34 GPa at 1 wt.% arc-MWNT [81]. This corresponds to a reinforcement of $dY/dV_f \sim 272$ GPa which is on a par with Cadek's value (scaled) for PVA composites. However, in this work no nucleation of crystallinity was observed. This suggests that good stress transfer can be obtained at an amorphous interface depending on the polymer.

Strength and modulus are not the only parameters that can be enhanced by incorporating nanotubes in a polymer matrix. Ruan et al. studied composites of CVD-MWNT in high density polyethylene [54]. They observed modest enhancement of the modulus from 0.98 GPa to 1.35 GPa with 1 wt.% MWNT ($dY/dV_f \sim 57$ GPa). An increase in strength from 8.3 MPa to 12.4 MPa was also observed. However, impressive results were achieved on alignment of the film by hot-drawing. As the draw ratio is increased modulus and strength increase at similar rates for both polymer and composite. By a draw ratio of 60–70, the

composites films had attained modulus and strength values of 50 GPa and 2.5 GPa respectively (cf. values of 60 GPa and 2 GPa for the polymer). However, the toughness increases much more rapidly for the composite films, reaching 150 MPa for a draw ratio of 70. This can be compared with a value of <50 MPa for the polymer. This represents a very tough material, 150 MPa is equivalent to ~100 J/g which is in the same range as Kevlar (Fig. 11).

In addition, Ruan et al. studied stress transfer from polymer to nanotube using Raman spectroscopy. They monitored the Raman shift of the D* band as a function of strain. The position of this band is known to be very sensitive to stress in the tube [145]. Significant red-shifts in the line position were observed, showing efficient stress transfer. In addition the polymer Raman modes at 1060 cm^{-1} and 1130 cm^{-1} (C–C stretches) were monitored. The positions of these modes are also sensitive to stress on the polymer backbone. While the position of both modes shifted significantly as a function of strain for the neat polymer, the shift was less pronounced for the composite. Again, this indicates that stress has been transferred from the polymer to the nanotubes for a given strain.

While it has been shown that both CVD-MWNT and arc-MWNT can be used to a greater or lesser degree to reinforce polymers, it is not clear what the optimum tube type is. This question was addressed by Cadek et al. in a paper in Nano Letters in 2004 [86]. They fabricated composites using polyvinylalcohol as a matrix filled with a range of different tube types: SWNT, DWNT, CVD-MWNT and arc-MWMT. They found that for all the nanotube types, except the SWNT, the reinforcement as represented by dY/dV_f scaled with the inverse nanotube diameter. This means that the composite Young's modulus scales directly with the total interfacial surface area in the film. However, for the SWNT composites the reinforcement was much lower than would be expected by this trend. This was explained as being due to slippage of SWNT in bundles. This work suggests that the optimum nanotubes for composite modulus enhancement are low diameter CVD-MWNT (Fig. 12).

This claim was put to the test shortly afterwards by Coleman et al. [48]. They fabricated PVA based composites using commercial low diameter (D ~15 nm) MWNT as a filler. They observed significant reinforcement with modulus enhancement from 1.92 GPa to 7.04 GPa at 0.6% nanotube volume fraction. This represents a reinforcement of $dY/dV_f = 754$ GPa. In addition strength enhancement from 81 MPa to 348 MPa was observed. In addition a microscopy study of composite fracture surfaces showed nanotube pullout. However, the pullout diameter showed that a layer of polymer had remained attached to the tube after fracture. The thickness of this layer was very similar to the measured thickness of a crystalline polymer coating nucleated by the MWNT. This strongly suggests that the presence of interfacial crystallinity has a large bearing on the mechanical properties of composites (Figs. 13 and 14).

While the focus for reinforcement has been on hard thermoplastics, some work has been done on the reinforcement of elastomers [82]. Dufresne et al. made composites

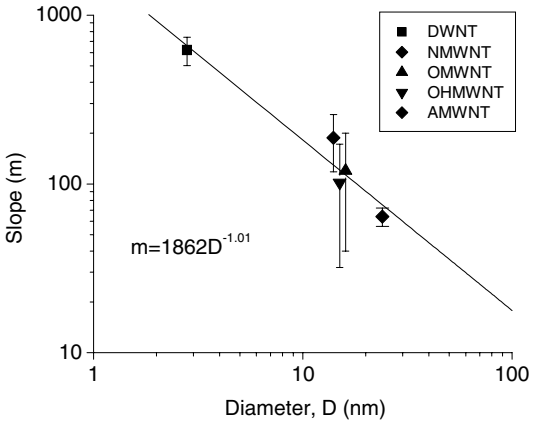

Fig. 12. Reinforcement levels in polyvinyl based composites as a function of nanotube diameter, D. In this work m is equivalent to dY/dV_f. The regression line shows that dY/dV_f scales with $1/D$. Reproduced from [86].

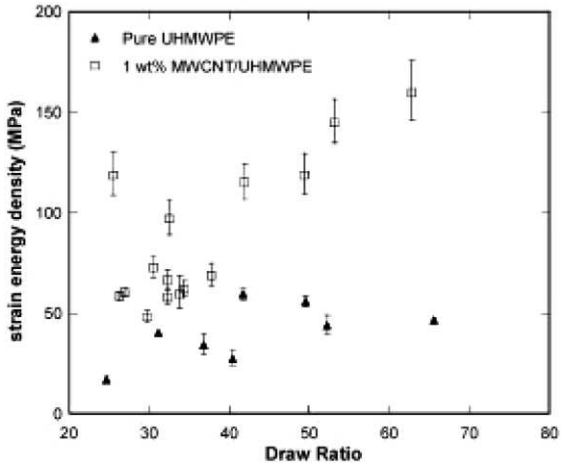

Fig. 11. Strain energy density (toughness) for drawn films of polyethylene and a polyethylene based composite as a function of draw ratio. Reproduced from [54].

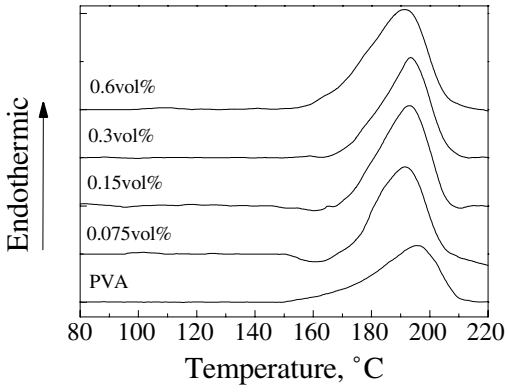

Fig. 13. Differential scanning calorimetry curves for a range of polyvinyl alcohol composites with different nanotube volume fractions. Note that the melt enthalpy increases with nanotube content. Reproduced from [48].

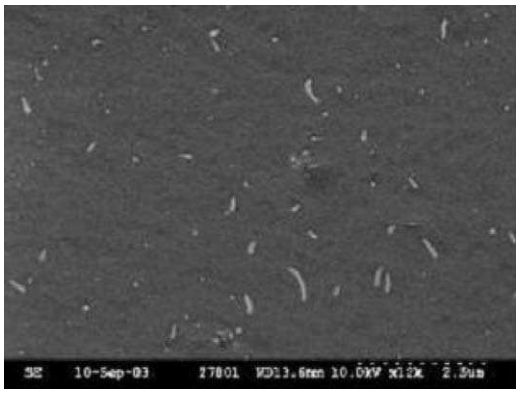

Fig. 14. SEM image of the fracture surface of a PVA CVD-MWNT based composite. Reproduced from [48].

from CVD-MWNT embedded in an amorphous polystyrene-co-butyl-acrylate latex. Measurements were made using both DMTA and tensile testing. They observed significant increases in modulus from 0.52 MPa to 3.54 MPa at 8.3 vol.%. However this actually represents relatively low reinforcement, $dY/dV_f \sim 35$ MPa, for the static measurements. In addition both the strain to break (ductility) and the tensile strength decreased with nanotube content.

6.2. Mechanical properties of melt processed composites

In this section we discuss mechanical properties of bulk composites fabricated by melt processing. All the results quoted for Young's modulus are summarised in Table 2.

Early work on the mechanical properties of bulk polymer nanotube composites was carried out by Jin et al. [91]. Testing PMMA doped with Arc-MWNT by DMA they observed an increase in Young's modulus from 0.7 GPa to 1.63 GPa at 17 wt.% nanotubes. This corresponds to a level of reinforcement of approximately 7 GPa which is similar to that achieved by Shaffer and Windle's first study. This was followed in 2002 by two studies on CVD-MWNT in polystyrene [92,98]. In these reports the modulus increased from ~2 GPa to 2.6 GPa and 4.5 GPa at 5 wt.% and 25 vol.%, respectively, providing reinforcement levels of 9 and 19 GPa. Interestingly enough, in both cases craze formation was observed in microscopy studies with nanotube pullout observed at the fracture surface. In one case [98] the nanotubes that had pulled out from the matrix were still coated with polymer, indicating the presence of very strong interfacial bonding.

Another study revealed small increases in the modulus of polycarbonate when mixed with CVD-MWNT ($dY/dV_f \sim 2.4$ GPa) [90]. Gorga et al. increased the stiffness of PMMA from 2.7 to 3.7 GPa on addition of 10 wt.% of CVD-MWNT ($dY/dV_f \sim 17$ GPa). In addition increases in strength from 64 to 80 MPa and a 170% increase in toughness were observed [95].

However, it was in 2004 that a number of researchers began to report significant improvements. Meincke et al. fabricated composites from CVD-MWNT in polyamide-6 [96]. This almost doubled the modulus, from 2.6 to 4.2 GPa at 12.5 wt.% corresponding to a reinforcement value of $dY/dV_f \sim 34$GPa. This was however accompanied by a significant reduction in ductility, from 40% to just 4%. In addition, they made blend composites from polyamide-6, ABS and nanotubes. Here the results were more modest with increases from 1.97 to 2.51 GPa at 7.5 wt.%. This gives a slightly lower reinforcement value of 11 GPa. However, this can be explained partly by the fact that the nanotubes were observed by TEM to reside only in the PA-6 phase. In the three phase blends the ductility fell from 105% to 40%, a fall that was accompanied by a decrease in impact strength by a factor of two.

Zhang and co-workers made composites from CVD-MWNT in polyamide6 [93,94]. They observed a threefold increase in modulus from 0.4 GPa to 1.24 GPa on addition of only 2 wt.% nanotubes corresponding to an impressive reinforcement value of $dY/dV_f \sim 64$ GPa. In addition, a significant increase in yield strength from 18 to 47 MPa was observed with similar increases in ultimate tensile strength. Furthermore, no decrease in toughness was observed as the ductility only fell slightly from 150% to 110%. These impressive results were attributed to very good dispersion and adhesion as observed by microscopy measurements (Fig. 15).

Finally, Manchado et al. blended small amounts of arc-SWNT into isotactic polypropylene [51]. They observed the modulus increase from 0.85 GPa to 1.19 GPa at 0.75 wt.%. In addition the strength increased form 31 MPa to 36 MPa

Table 2
Moduli of melt processed bulk matrices and their composites

Nanotube Type	Polymer	Y_{Poly} (GPa)	Y_{Max} (GPa)	Max NT content	dY/dV_f (GPa)	Comment	Reference and year
Arc-MWNT	PMMA	0.73	1.63	17 wt.%	~7	DMA	[91] 2001
CVD-MWNT	PS	2	4.5	25 vol.%	~10	TT	[92] 2002
CVD-MWNT	PS	2.3	2.6	5 wt.%	~9	DMA	[98] 2002
CVD-MWNT	PC	0.8	1.04	15 wt.%	~2.4	DMA	[90] 2003
CVD-MWNT	PMMA	2.7	3.7	10 wt.%	~17	TT	[95] 2004
CVD-MWNT	PA6	2.6	4.2	12.5 wt.%	34	TT	[96] 2004
CVD-MWNT	PA6/ABS	1.97	2.51	7.5 wt.%	11		
CVD-MWMT	Nylon	0.4	1.24	2 wt.%	64	TT	[93] 2004
Arc-SWNT	PP	0.85	1.19	0.75 wt.%	68	TT	[51] 2005

The abbreviations DMA and TT refer to dynamic mechanical analysis and tensile testing, respectively.

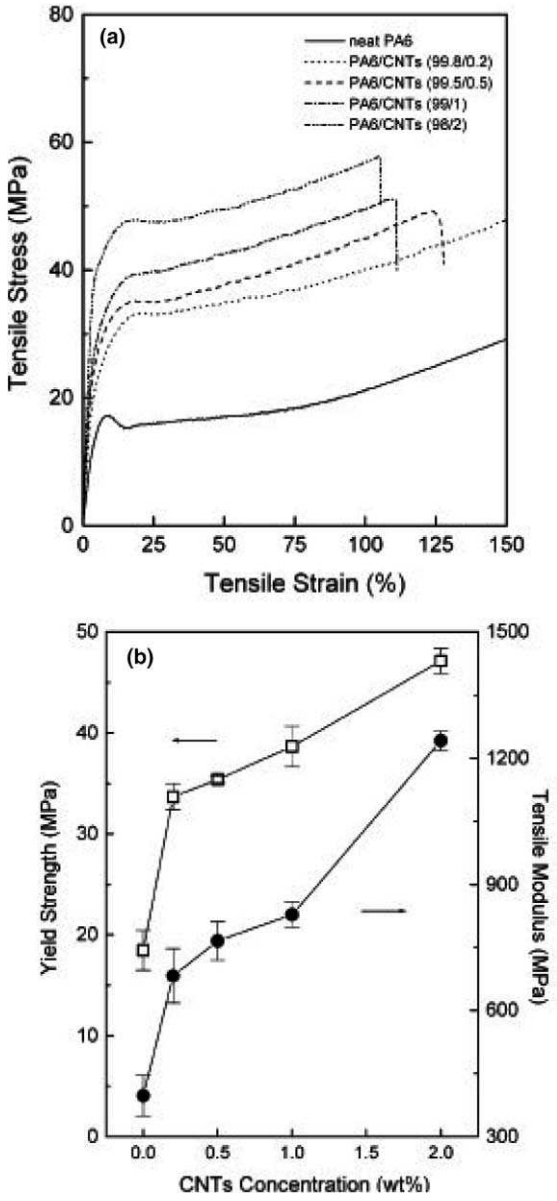

Fig. 15. (a) Stress–strain curves and (b) yield strength and modulus for PA6-MWNT composites. Reproduced from [93].

by 0.5 wt.%. Both properties were observed to fall off at higher loading levels. The ductility only dropped marginally from 493% to 402% meaning that inclusion of nanotubes did not result in any significant toughness reduction. This work corresponds to a reinforcement value of $dY/dV_f \sim 68$ GPa.

6.3. Mechanical properties of melt processed fibres

Some promising mechanical results have been reported for melt processed composite fibres. These will be reviewed in this section with all the results for Young's modulus summarised in Table 3.

In 2000, Haggenmueller et al. reported on melt processed fibres spun from PMMA and SWNT for a wide range of draw ratios [100]. The maximum modulus observed was 7 GPa for a draw ratio of ~100. Fibre strength was observed to scale with draw ratio to a maximum of 130 MPa at a high draw ratio of ~900. A typical value of reinforcement was $dY/dV_f \sim 57$ GPa for a draw ratio of ~70. Nanotubes alignment within the fibres was measured by Raman spectroscopy. For the higher draw ratios significant alignment was observed with an orientation distribution as low as 4° measured for a draw ratio of 300.

Fibres fabricated from PP and SWNT were studied by Kearns and Shambaugh [101] in 2002. The fibres were post-drawn after spinning which resulted in excellent mechanical properties. They saw increases in modulus from 6.3 to 9.8 GPa on addition of 1 wt.% SWNT which corresponds to a reinforcement value of $dV/dV_f \sim$ 530 GPa. However, the strength increased from an already impressive value of 709 MPa to 1027 MPa upon addition of 1 wt.% SWNT at a draw ration of 8. This high strength is already good enough for a range of applications. In addition the strain to break actually increased from 19% to 27% on the introduction of nanotubes. This means that the fibres actually toughen when nanotubes are added.

In an extension of this work, the same group made fibres containing SWNT from two types of PP, a high (HMFR) and a low melt flow rate polymer (LMFR) [102]. In both cases increases in modulus were observed with reinforcements of ~179 and ~285 GPa for the LMFR and HMFR PP, respectively. However, while increases in strength,

Table 3
Moduli of melt processed fibres

Nanotube type	Polymer	Y_{Poly} (GPa)	Y_{Max} (GPa)	NT content (wt.%)	dY/dV_f (GPa)	Comment	Reference and year
SWNT	PMMA	3.1	6.0	6	~57	TT	[100] 2000
SWNT	PP	6.3	9.8	1	~530	TT	[101] 2002
SWNT	LMFR PP	0.91	2.09	1	~179	DMA	[102] 2004
	HMFR PP	1.47	3.35	1	~285	DMA	
SWNT	PP	0.4	1.4	5	~38	TT	[146] 2005
CVD-MWNT	PS	1.2	3.0	5	~36	TT	[92] 2002
Arc-MWNT	PA6	0.8	0.95	10	~2	TT	[103] 2004
CVD-MWNT		0.8	1.4	5	~10.6	TT	
CVD-MWNT		0.8	1.6	10	~10.2	TT	

The abbreviations DMA and TT refer to dynamic mechanical analysis and tensile testing, respectively.

toughness and ductility were observed for the LMFR polymer, the opposite was true for the HMFR material. This is an important point as it shows clearly that subtle differences in polymer type can have significant impact of the potential for reinforcement.

PP-SWNT fibres have also been fabricated by Chang et al. [146]. In this case, significant increases in modulus from 0.4 to 1.4 GPa ($dY/dV_f \sim 38$GPa) were observed. In addition, the strength tripled on the addition of 5 wt.% SWNT. Raman measurements were used to show significant stress transfer between polymer and tube. However, no increase in modulus or orientation was observed as a function of draw ratio. This is important as it shows that a fuller understanding of post-treatment processes is needed before results equivalent to those of Kearns et al. are routine.

Some work has also been carried out on polymer-MWNT melt-spun fibres. Andrews et al. saw increases in modulus from 1.2 to 3 GPa on the addition of 5 wt.% CVD-MWNT to PS [92]. This represents a reinforcement value of $dY/dV_f \sim 36$ GPa.

Finally Sandler et al. [103] carried out a comparative survey on the properties of composite fibres spun from polyamide-12 with a range of different types of MWNT. Arc-MWNT were shown to have the worst reinforcement properties, probably due to the high level of impurities present. Significantly better results were obtained for both aligned and entangled CVD-MWNT with increases in modulus by factors of ×1.75 and ×2, respectively. Strength increases from a value of 22 MPa for the polymer to 30 and 47 MPa for the composites containing aligned and entangled tubes, respectively, were also observed. While these figures make the entangled tubes appear better, the ductility only decreased marginally for the aligned nanotubes compared to a large reduction from 400% to 160% for the entangled tubes. This shows that while the entangled tubes may be marginally more favourable for strength and stiffness applications, the aligned nanotubes may be superior for energy absorption.

6.4. Mechanical properties of composites based on thermosetting polymers

Due to their wide range of industrial uses, thermosetting polymers in general and epoxy resins in particular have been widely studied as a potential matrix for nanotube based composites. In this section all matrices were epoxy resins unless otherwise stated. Details of the matrix and a summary of the modulus values are given in Table 4.

The first record of the formation of epoxy-nanotube composites comes from a paper by Ajayan in 1994 [147]. In this work nanotubes were aligned within the epoxy matrix by the shear forces induced by cutting with a diamond knife. However no quantitative mechanical measurements were made.

The first true mechanical study was made by Schadler et al. in 1998 [53]. They measured the stress–strain properties of a MWNT–epoxy composite in both tension and compression. In tension the modulus increased from 3.1 GPa to 3.71 GPa on addition of 5 wt.% nanotubes, a reinforcement of $dY/dV_f = 18$ GPa. However better results were seen in compression with an increase in modulus from 3.63 to 4.5 GPa which corresponds to a reinforcement of 26 GPa. No significant increases in strength of toughness were observed. The difference between tension and compression was explained by Raman studies which showed significantly better stress transfer to the nanotubes in compression than in tension. This can be explained by the fact that load transfer in compression can be thought of as a hydrostatic pressure effect while load transfer in tension relies on the matrix nanotube bond. However it should be pointed out that later studies showed the reverse to be true, i.e. load transfer in tension but none in compression [52].

A number of other studies have observed moderate increases in modulus but either no increase or a significant decrease in strength and toughness [104,107]. On the other hand Xu et al. observed a significant increase in modulus from 4.2 to 5 GPa at only 0.1 wt.% MWNT [106]. This

Table 4
Moduli of thermoset polymer matrices and that of their respective composites

Nanotube type	Resin/hardener	Y_{Poly} (GPa)	Y_{Max} (GPa)	NT content (wt.%)	dY/dV_f (GPa)	Comment	Reference and year
MWNT	Shell EPON 828/triethylene tetraamine	3.1 (3.63)	3.71 (4.5)	5	~18 (~26)	TT, tension (compression)	[53] 1998
CVD-MWNT	EPON SU-8	4.2	5.0	0.1	~1200	Shaft loaded blister method	[106] 2002
CVD-MWNT	Bisphenol A-epichlorhydrine/ triethylenetetramine	0.118	0.465	4	~13	TT	[148] 2002
CVD-MWNT	Bisphenol A-epichlorhydrine/ triethylenetetramine	1.2	2.4	1	~330	TT	[150] 2003
MWNT	D.E.R. 736 P/D.E.H. 24, Dow Chemical	1.4×10^{-3}	2.1×10^{-3}	0.25	~0.5	TT	[104] 2004
CVD-MWNT	Polyimide triple A PI	2.84	3.9	14.3	~11	TT	[107] 2004
CVD-MWNT	LY 5052 CIBA-GEIGY/ HY5052CIBA-GEIGY	2.75	4.13	6	~45	TT	[149] 2004
SWNT	1,1-Bis(4-cyanatophenyl)ethane	4	7	5	~94	NHT	[151] 2004

The abbreviations NHT and TT refer to nanohardness testing and tensile testing, respectively.

corresponds to a massive reinforcement value of $dY/dV_f \sim 1200$ GPa. According to the rule of mixtures this value is close to the maximum possible reinforcement for a material filled with perfectly aligned, well-dispersed nanotubes displaying perfect stress transfer. As these measurements were made by flexural testing using the Shaft loaded blister method, it would be interesting to see them confirmed using tensile testing.

Allaoui et al. obtained good all-round properties for CVD-MWNT–epoxy composites in 2002 [148]. They measured an increase in modulus from 0.12 GPa to 0.47 GPa on addition of 4 wt.% nanotubes, a reinforcement of 13 GPa. This was accompanied by a doubling in strength from 5 to 10 MPa and a reduction in ductility from 20% to 10%. This resulted in a small toughening of the material.

Further work was carried out on CVD-MWNT–epoxy composites by Breton et al. Significant increases in modulus from 2.75 GPa to 4.13 GPa were observed on addition of 6 wt.% nanotubes corresponding to $dY/dV_f \sim 45$ GPa. They attributed the large reinforcement values to residual oxygen containing groups that had covalently bonded to the nanotubes during purification. The presence of these groups may have improved interfacial bonding [149]. Bai et al. observed a doubling of Young's modulus from 1.2 to 2.4 GPa on addition of 1 wt.% CVD-MWNT. This corresponds to a reinforcement value of $dY/dV_f \sim 330$ GPa which is the largest observed for an epoxy-based composite as measured by tensile testing. In addition, significant increases in strength from 30 to 41 MPa were recorded. Excellent matrix–nanotube adhesion was confirmed by the observation of nanotube breakage during fracture surface studies [150].

Finally Li et al. [151] studied SWNT–epoxy composites by nanohardness testing. They observed an increase in modulus from 4 to 7 GPa with 5 wt.% SWNT ($dY/dV_f \sim 94$ GPa). Increases in hardness from 0.35 to 0.45 GPa were also observed.

6.5. Mechanical properties of composites filled with chemically reacted nanotubes

In this section we will discuss composites where chemical reactions have been used either in the formation of the composite or as a method to treat the nanotubes. This section has been divided into subsections. The first deals with cases where composite formation at least partially involved the in situ polymerisation of the polymer in the presence of nanotubes. The second section describes composites where the nanotubes were initially chemically modified. Composite formation was then typically by one of the methods described in Section 5.

6.5.1. Mechanical properties of composites polymerised in the presence of nanotubes

In situ polymerisation has a number of advantages over other composite formation methods. It is easier to get intimate interactions between polymer and nanotube during the growth stage than afterwards. In addition, depending on how the reaction is carried out some of the polymer strands can be covalently attached to the nanotubes. These methods are expected to achieve large interfacial shear strength because of the strong, even covalent, polymer nanotube interaction.

An early study into the in situ polymerisation of PMMA in the presence of CVD-MWNT was carried out by Jia et al. [120]. While stiffness data was not given, the strength increased from 55 to 72 MPa at 5 wt.%. This was accompanied by marginal increases in toughness and hardness. Shortly afterwards Park et al. reacted SWNT with polyamide precursors to form a PI-SWNT composite [126] An increase in stiffness from 1 GPa to 1.6 GPa was observed at 1 vol.% SWNT, corresponding to $dY/dV_f \sim 60$ GPa.

A breakthrough, however, came in a paper by Kumar et al. [123]. They polymerised PBO in the presence of SWNT before wet-spinning fibres. The PBO modulus of 138 GPa was increased to 167 GPa on addition of 10 wt.% SWNT, a reinforcement value of ~550 GPa. In addition the fibre strength was improved from 2.6 GPa to 4.2 GPa. While this does not match the strength of commercial PBO fibres (~6 GPa),[2] it is certainly an impressive start. Furthermore, incorporation of SWNT actually increased the ductility, thereby improving the toughness which is an important consideration for fibre materials.

In another study by Velasco-Santos et al., PMMA was polymerised in the presence of arc-MWNT [121]. This is important as they have higher intrinsic strength or stiffness than CVD-MWNT or bundles of SWNT. Stiffness was increased from 1.5 to 2.5 GPa by 1 wt.% MWNT, corresponding to $dY/dV_f \sim 150$ GPa. In addition, the strength increased from 30 to 50 MPa with a proportional increase in toughness.

Finally, Putz et al. [122] in another study on PMMA and SWNT observed an increase in stiffness as measured by DMA from 0.3 to 0.38 GPa. However this increase occurred at the extremely low volume fraction of 8×10^{-5}. This corresponds to a reinforcement value of $dY/dV_f \sim 960$ GPa. This is close to the theoretical rule of mixtures maximum for long, well-aligned, well-graphitised nanotubes. However it should be pointed out that this study was carried out at 100 rad/s which is a reasonably high frequency. Time-temperature equivalence of mechanical properties for visco-elastic materials suggests that this may be an overestimate as compared to values obtained by pseudo-static measurements [152]. These results are listed in Table 5.

6.5.2. Mechanical properties of composites based on functionalised nanotubes

Composites based on functionalised nanotubes are expected to have large interfacial shear strengths. Covalently grafted long-chain molecules entangle with the polymer matrix creating a very strong bond. In addition the

[2] http://www.toyobo.co.jp/e/seihin/kc/pbo/.

Table 5
Mechanical properties of in situ polymerised composites

Nanotube type	Matrix	Y_{Poly} (GPa)	Y_{Max} (GPa)	NT content	dY/dV_f (GPa)	Comment	Reference and year
In situ polymerisation							
SWNT	PI	1.0	1.6	1 vol.%	~60	DMA	[126] 2002
SWNT	PBO	138	167	10 wt.%	~550	TT	[123] 2002
Arc-MWNT	PMMA	1.5	2.5	1 wt.%	~150	TT/DMA	[121] 2003
SWNT	PMMA	0.3	0.38	0.01 wt.%	~960	DMA@100 rad/s	[122] 2004
Functionalisation							
CVD-MWNT/octadecylamine	P(MMA-co-EMA)	1.64	2.62	10 wt.%	~15	TT	[143] 2004
CVD-MWNT/Cl-PP	Cl-PP	0.22	0.68	0.6 vol.%	72	TT	[142] 2004
SWNT/large organic groups	Epoxy	2.02	3.4	4 wt.%	~95	TT	[128] 2004
Arc-MWNT/PMMA	PMMA	2.9	29	20 wt.%	~115	DMA	[135] 2004
SWNT/PA6	PA6	0.44	1.2	1.5 wt.%	~120	TT	[125] 2005
SWNT/OH	PVA	2.4	4.3	0.8 wt.%	305	TT	[141] 2005
CVD-MWNT/ferririn protein	PVA	3.4	7.2	1.5 wt.%	~380	DMA	[140] 2005

The abbreviations DMA and TT refer to dynamic mechanical analysis and tensile testing, respectively.

functional groups act to make the nanotubes more compatible both with polymer hosts and solvents. This tends to dramatically improve the nanotube dispersion and hence further improve composite properties.

Yang et al. [143] fabricated composites from CVD-MWNT in p(MMA-co–EMA). The stiffness increased from 1.64 to 2.62 GPa on introduction of 10 wt.% nanotubes ($dY/dV_f \sim 15$ GPa). While the strength also increased form 55 to 73 MPa, the material became very brittle at higher nanotube contents. Furthermore there was no significant difference between functionalised and pristine nanotubes. Blake et al. (Fig. 16) covalently attached chlorinated PP to CVD-MWNT [142] and blended with chlorinated PP. Stiffness increased from 0.22 to 0.68 GPa, corresponding to a reinforcement of 72 GPa. Moreover both strength and toughness increased from 12.5 to 49 MPa and from 24 to 108 J/g, respectively.

In two papers Zhu et al. demonstrated covalent grafting of large organic molecules to SWNT [127,128]. These were then dispersed in epoxy resin and treated to covalently attach the functionalities to the resin. The modulus

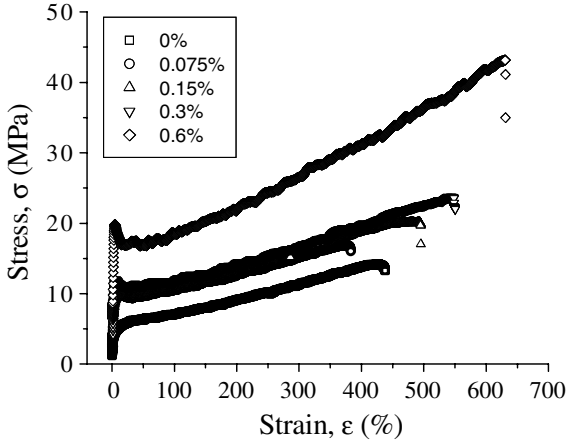

Fig. 16. Stress–strain curves for a range of composites fabricated from functionalised MWNT and CL-polypropylene. Reproduced from [142].

increased from 2.02 to 3.4 GPa on addition of 4 wt.% SWNT ($dY/dV_f \sim 95$ GPa). In addition the strength improved from 83 to 102 MPa. The high level of stress transfer was suggested by the fact that many tubes fractured on composite failure.

Hwang et al. reinforced PMMA by the addition of PMMA grafted arc-MWNT [135]. They observed an increase in modulus as measured by DMA from 2.9 to 29 GPa on addition of 20 wt.% nanotubes ($dY/dV_f \sim 115$ GPa). This is significant for two reasons. First they managed to successfully functionalise arc-MWNT which is challenging compared to functionalisation of CVD-MWNT. This means that the fillers have very high modulus. In addition, good dispersion and a continued increase in modulus enhancement was observed up to 20 wt.%, which is unprecedented. Failure of the nanotubes by the "sword and sheath" method was observed suggesting good interfacial stress transfer (Fig. 17).

Melt-spun fibres from PA6 grafted SWNT in a PA6 matrix were produced by Gao et al. [125]. The fibres were stiffened from 440 MPa to 1200 MPa on addition of 1.5 wt.% tubes ($dY/dV_f \sim 120$ GPa). The strength was doubled from 41 to 86 MPa.

Liu et al. reinforced PVA with hydroxyl functionalised SWNT [141]. The idea was that the –OH groups would hydrogen bond with the –OH of the PVA. Reasonably good modulus enhancement was observed with an increase from 2.4 to 4.3 GPa on addition of 0.8 wt.% nanotubes, corresponding to a reinforcement value of ~305 GPa. A strength increase from 74 to 107 MPa was also observed. These results were explained by the observation of good load transfer by Raman spectroscopy.

Finally, a slightly different type of functionalisation was demonstrated in 2005. The protein, ferratin, was successfully grafted onto CVD-MWNT [140]. This material was mixed with PVA. The authors claimed that the ferratin was expected to bond with the PVA. Indeed, significant modulus enhancement from 3.4 to 7.2 GPa was observed corresponding to a reinforcement of 380 GPa.

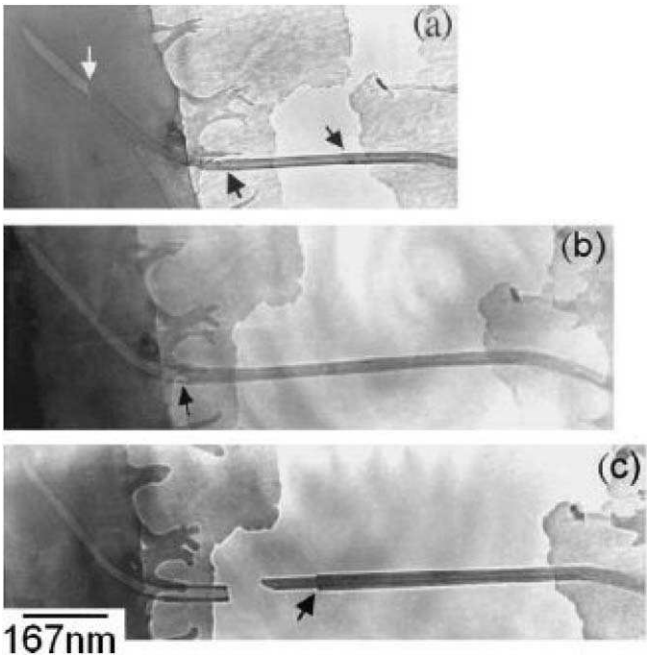

Fig. 17. TEM images showing failure of a MWNT bridging a gap in a composite film as can be seen in (c) the nanotube fails by the sword and sheath mechanism. Reproduced from [135].

6.6. Mechanical properties of novel composites

A number of novel processing techniques have been described in the literature and summarised in the processing section. Here, we will explore the mechanical properties of composites made using these techniques.

6.6.1. Infiltration methods

These techniques have focused on improving the mechanical properties of existing nanotubes based structures by infiltrating polymer from solution to act as a binding agent. Coleman et al. infiltrated PVA, PVP and PS into Buckypaper [108]. They found increases in modulus, strength, toughness and strain to break for the infiltrated papers. At maximal loading levels of approximately 30 wt.% polymer the modulus, strength and toughness increased by factors of ×3, ×9 and ×28, respectively. This was attributed to improvements in interbundle load transfer by polymer bridging. There were slight differences in load transfer with PS > PVP > PVA in agreement with their relative lypophilicities. In a further study, Frizzel et al. showed that infiltration of high molecular weight molecules was better for improving modulus and strength while lower molecular polymers were optimal for the improvement of toughness. This was attributed to variations in chain conformation related to the intercalation process [153]. In a similar study Wang et al. demonstrated sevenfold improvements in Buckypaper stiffness by intercalation of epoxy resulting in Young's modulus of up to 15 GPa [109].

Lahiff et al. [154] infiltrated PDMS into a MWNT forest by spin coating. Increases in modulus by a factor of two were observed although the film was weaker and more brittle than neat PDMS. The small value of reinforcement was attributed to poor stress transfer.

These infiltration methods are potentially important as they could be used to enhance the mechanical properties of nanotube fibres [155,156] or sheets [157].

6.6.2. Layer by layer deposition methods

Composites consisting of alternating layers of nanotubes and polyelectrolyte have shown great promise as high strength light weight materials. Mamedov demonstrated such materials from SWNT and poly(ethyleneimine) (PEI) [111]. Compared to PEI, significant increases in modulus, from 0.3 GPa to ~11 GPa were observed for composites containing ~50 wt.% SWNT. Increases in strength from ~9 MPa to up to 325 MPa were observed. While the composites were less ductile than the neat polymer (1% versus 4%), toughness still increased by a factor of five to ten.

In a similar study, Olek et al. [112] fabricated layer by layer composites using MWNT and PEI. Two types of MWNT were used, "hollow" and "bamboo". The bamboo composites displayed moduli and strengths of ~4.5 GPa and ~150 MPa, respectively. The hollow MWNT composites showed slightly lower values of ~2 GPa and ~110 MPa, respectively. To further emphasise the importance of tube type and quality, hollow nanotubes were boiled in nitric acid before composite fabrication. This resulted in much lower modulus and strength values of ~0.2 GPa and 35 MPa, respectively.

6.6.3. Coagulation spun fibres

In 2000, Vigolo et al. demonstrated that composite fibres could be spun by coagulation spinning. However care was taken to remove the polymer post-spinning. These fibres displayed reasonable moduli and strength of 9–15 GPa and ~150 MPa, respectively [114]. They were extremely flexible and could easily be tied into knots. The mechanical properties of these fibres could be significantly improved by stretching when wet. This tended to align the nanotubes resulting in moduli of ~40 GPa and strengths of up to 230 MPa [158] (Fig. 18).

However Dalton et al. demonstrated in 2003 that the properties could be markedly improved by leaving the polymer in the fibre [115,160]. This resulted in large increases in Young's modulus and strength to 80 GPa and 1.8 GPa, respectively. In addition these fibres could be stretched until strains of ~100% resulting in massive toughness values of up to 570 J/g which is an order of magnitude larger than Kevlar. Miaudet et al. [116] have recently shown that toughness values as high as 870 J/g and 690 J/g can be achieved for similar fibres spun from SWNTs and MWNTs, respectively. In addition by drawing the fibres at elevated temperature they have shown that SWNT based fibres with excellent all-round properties can be obtained. These fibres had moduli, strength and toughness values of 45 GPa, 1.8 GPa and 55 J/g. Crucially, this toughness value was obtained at the low strain value of 11%.

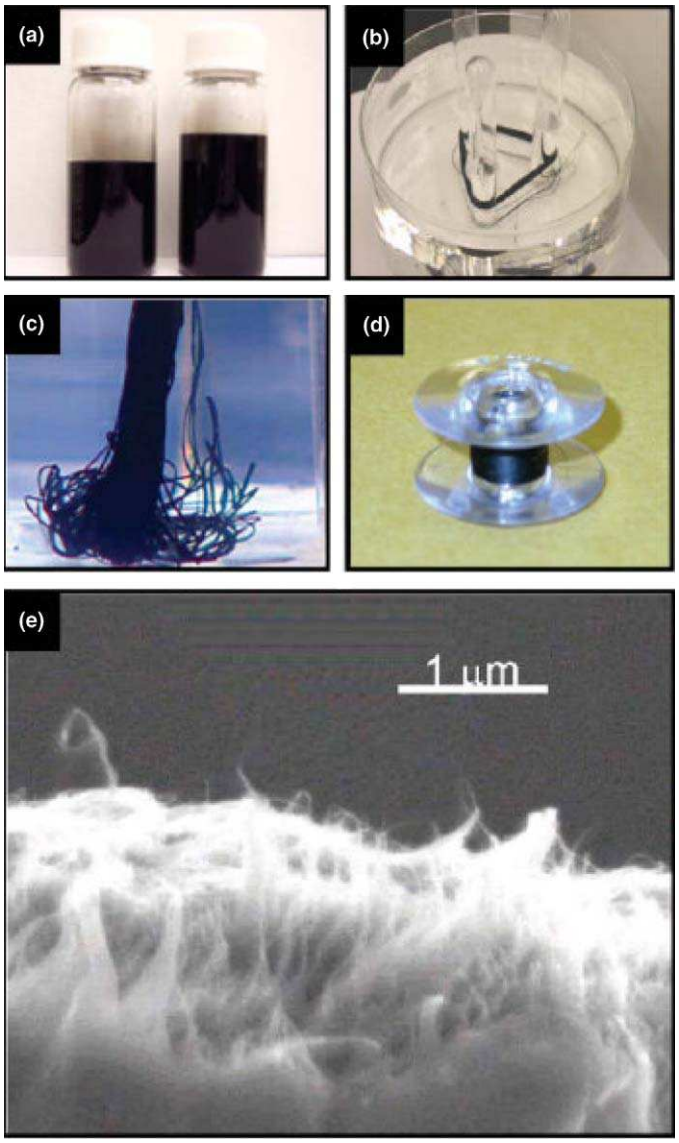

Fig. 18. (a) Stable SWNT suspension in a lithium dodecyl sulfate/dionized water solution. These suspensions are used as the "ink" for spinning nanotube gel fibres. (b) The ink in (a) is injected into a glass pipe (where the coagulation solution is coaxially flowing) to form the gel fibre, which travels along the glass pipe and is eventually collected on a rotating mandrel in a water bath. A hundred meters of gel state fibre tightly wrapped on a mandrel is shown. (c) These pictured gel fibres act like a rubber, reversibly elongating up to 400% before breaking. (d) The gel is subsequently drawn out of the bath, passed over a series of godets and through an acetone washing bath during a drying process, and finally wound onto a spool (pictured, with a wound nanotube fibre). (e) Scanning electron micrograph of the end of an undrawn composite carbon nanotube fibre, showing carbon nanotubes in a polyvinyl alcohol matrix. Reproduced from [159].

Fibres made from SWNT and PVA have also been spun using DNA as a dispersant. These materials demonstrated moduli in the range 12–18 GPa and strengths of 90–110 MPa [161].

6.6.4. Electrospun fibres

Composite fibres have also been produced by electrospinning. Ko et al. demonstrated stabilized PAN/SWNT fibres with significantly increased Young's modulus [118]. Fibre modulus was 140 GPa at 4 wt.% nanotubes, which compares well with the PAN fibre modulus of 60 GPa. However it should be pointed out that these measurements were carried out in compression using an AFM. Sen et al. [119] built up membranes from electrospun fibres of SWNT and polyureathane. These could then be characterised by tensile testing. Polyureathane fibres had moduli and strengths of 7 MPa and 7 MPa, respectively. However the membranes fabricated from composite fibres demonstrated moduli and strengths of up to 25 and 15 MPa.

7. Discussion

Shown in Table 6 is a summary of the mechanical results discussed in the previous sections for each composite preparation type. The values shown represent the mean and median reinforcement values. In addition the maximum value reported in each section is shown for composites based on both SWNTs and MWNTs. Finally the maximum reported values for modulus and strength are also shown.

The most obvious result here is that composites based on chemically modified nanotubes show the best results. This is not surprising as functionalisation, for example, should significantly improve both dispersion and stress transfer. While the results for solution based composites are also impressive, they are biased by the high crystallinity PVA based composites [48,86]. While these undoubtedly show significant reinforcement, much of this is due to crystallinity nucleation which cannot be relied upon for all polymer matrices. However, specific effects due to the details of the solution based polymer nanotube interaction may result in a better interface. This fact needs clarification.

A salient message is the low reinforcement observed for the melt processed composites. While the fibres display better reinforcement compared to the bulk, the difference is consistent with alignment effects. Of all the processing methods, the overall results are worst for the melt based

Table 6
Summary/comparison of reinforcement of SWNT and MWNT-composites fabricated by various processes

	Solution	Melt	Melt (fibre)	Epoxy	In situ poly	Functionalisation
Mean dY/dV_f (GPa)	309	23	128	231	430	157
Median dY/dV_f (GPa)	128	11	38	18	60–150	115
Max dY/dV_f (GPa) SWNT	112	68	530	94	960	305
Max dY/dV_f (GPa) MWNT	1244	64	36	330	150	380
Max Y (GPa)	7	4.5	9.8	4.5	167	29
Max σ (MPa)	348	80	1032	41	4200	107

systems. While the results for the epoxy based systems are slightly better, these are not brilliant either.

It should be pointed out though that the best results reported are actually very good. Both rule of mixtures and the Halpin–Tsai equations (taking $Y_m \sim 1$GPa and $l/D \sim 1000$) predict maximum dY/dV_f values of approximately 1 TPa. A number of the systems studied report values in this range [48,101,122].

We can also compare SWNT versus MWNT based composites. Table 6 shows that the best reinforcement occurred for MWNT based composites in half the categories. This shows it is premature to assume that SWNT are superior as many commentators have.

Another disappointing fact is that strength enhancement has been poor except in the case of composite fibres. Given that high strength is one area where nanotubes retain significant advantages over carbon fibres, this is unexpected and must be addressed.

These results suggest that there are three main areas where significant improvement is urgently needed. As suggested previously, the problems with mechanical reinforcement of melt processed composites must be addressed. Any nanotube reinforced composites produced at an industrial level are likely to be produced by melt processing. It is likely that the problems are based on dispersion or interfacial shear strength issues. If this is the case, these may be addressed by functionalisation of the nanotubes. This will result in them being more compatible with the polymer melt and so improve dispersion. In addition IFSS will be improved for the reasons discussed above.

Another significant problem is the disappointing values for composite strength. A more important issue is probably a partial cause of this. In very few cases are large volume fractions attained. One notable exception is the work of Hwang where the modulus increased up to 20 wt.%. This resulted in by far the highest modulus for bulk composites. It is imperative that high volume fraction composites with good dispersion can routinely be made.

How do we address these issues? One possibility is to optimise the nanotube type. The most obvious question is SWNT versus MWNT? Here the high volume fraction issue may provide an answer. Imagine we could routinely produce individual, isolated SWNT dispersed in a composite. In that situation we can easily calculate that for $V_f = 1\%$, every polymer strand would be within 5 nm of a nanotube. This is within one radius of gyration and must surely be very close to an upper bound for volume fraction [162]. While much higher volume fractions have been attained, all SWNT exist in bundles under these conditions. Under these circumstances SWNTs lose their intrinsic advantages.

In the case MWNT with diameters of ~10 nm however, even at $V_f = 10\%$, nanotubes are on average separated by 20 nm. This gives us much more scope to attain high volume fractions with MWNT. The volume fraction at which every polymer strand is within 5 nm of a nanotube is a massive 25 vol.%. Thus in the ideal world arc-MWNT would be the obvious choice as the ultimate filler. However, compared to CVD-MWNT they are very expensive and difficult to functionalise. A better option would be to look for some cheap method to improve the graphitisation of CVD-MWNT.

Length and diameter can also be optimised. In order to maximise composite strength and stiffness, long tubes are required. Assuming an interfacial shear strength of 50 MPa and a strength of 50GPa for SWNT and arc-MWNT and 10 GPa for CVD-MWNT we can calculate the critical length in each case using Eq. (2). These work out as ~1 μm for arc-MWNT, ~100–500 nm for CVD-MWNT and ~400 nm for SWNT. In order to maximise reinforcement we will need nanotubes with lengths several times the critical length, possibly as long as 5 μm. However, long tubes are very hard to disperse properly, so we will be faced with a trade-off. Similarly, low diameter nanotubes give rise to greater surface area allowing the maximisation of interaction with the matrix. However for reasons already discussed, if the diameter gets too small, the maximum nanotubes loading level will be compromised. For these reasons there must be an optimum diameter and length.

Once we have identified the optimum tube type we must maximise nanotube solubility, dispersion (and hence volume fraction) and stress transfer. Fortunately all these factors can be addressed as one by functionalisation of the nanotubes. Choice of the right functional group will optimise interactions with either the solvent or the melt and aid stress transfer. In order to perfect the functionalisation scheme, there are three aspects to consider. The molecular structure of the group must be chosen. This may for example be a short chain analogue to the host polymer. In addition the group length and surface density would be expected to effect dispersion and stress transfer. However care must be taken that high levels of functionalisation do not severely degrade the intrinsic mechanical properties of the nanotubes.

Once the nanotubes have been fully optimised we can consider what mechanical properties are attainable. We will calculate these properties for a typical thermoplastic with low intrinsic modulus and strength. Assuming that the optimum tube length is a few times the critical length we can be confident that the length efficiency factors for both modulus and length will both approach 1 allowing us to use Eqs. (1) and (7) for composite modulus and strength. We will assume that the upper limit for SWNT loading is 1 vol.% (as discussed) and that $Y_{SWNT} = 1$ TPa and $\sigma_{SWNT} = 50$ GPa. Then for an aligned composite $Y_C \sim 10$GPa and $\sigma_C \sim 0.5$GPa.

We can do significantly better for arc-MWNT. We can assume a conservative upper limit for volume fraction at 20 vol.% as discussed above. Then taking $Y_{MWNT} = 1$ TPa and $\sigma_{MWNT} = 50$ GPa as for SWNT we get $Y_C \sim 200$GPa and $\sigma_C \sim 10$GPa for an aligned composite. While these numbers are significantly better than those for SWNT, they represent an upper limit. Real applications will almost certainly use CVD-MWNT which have poorer mechanical properties. If we assume for CVD-MWNT, $Y_{MWNT} =$

300 GPa and $\sigma_{MWNT} = 10$ GPa, which seem reasonable then we can achieve $Y_C \sim 60$GPa and $\sigma_C \sim 2$GPa for an aligned composite. While these values are not earth shattering, they are respectable. They represent a stiffness equivalent to that of aluminium and a strength comparable to hardened steel. In addition they should be considered lower bounds. By careful functionalisation it may be possible to push the maximum volume fraction beyond 20 vol.%. In addition the intrinsic properties of CVD-MWNT can probably be improved by high temperature annealing in analogy to vapor grown carbon fibres. The challenge will be to find a cost effective way to achieve this.

8. Conclusion

In conclusion, much progress has been made over the last few years in composite reinforcement using carbon nanotubes. Reinforcement levels are creeping towards those levels predicted by theory. In addition, many researchers are branching out with the fabrication of novel structures by innovative processing techniques. Some of these materials, such as coagulation spun fibres have even challenged state of the art materials such as Kevlar. Most importantly, the overriding problems of dispersion and stress transfer are being addressed using chemical techniques such as functionalisation. If this progress continues apace, we can expect a continuing bright future in this fascinating and potentially very useful area.

Acknowledgement

The authors would like to thank Milo Shaffer and Brian Grady for useful discussions. In addition, we are grateful to Leslie Carpenter for proofreading the manuscript and providing many useful comments. Financial help from the Embark Initiative, operated by the Irish Research Council for Science, Engineering and Technology (IRCSET) is appreciated (JNC).

References

[1] Baughman RH, Zakhidov AA, de Heer WA. Carbon nanotubes—the route toward applications. Science 2002;297(5582):787–92.
[2] Cao J, Wang Q, Rolandi M, Dai H. Aharonov–Bohm interference and beating in single-walled carbon-nanotube interferometers. Phys Rev Lett 2004;93(21):1–4.
[3] Kilbride BE, Coleman JN, Fraysse J, Fournet P, Cadek M, Drury A, et al. Experimental observation of scaling laws for alternating current and direct current conductivity in polymer–carbon nanotube composite thin films. J Appl Phys 2002;92:4024–30.
[4] Biercuk MJ, Llaguno MC, Radosavljevic M, Hyun JK, Johnson AT. Carbon nanotube composites for thermal management. Appl Phys Lett 2002;80(15):2767–9.
[5] Callister WD. Materials science and engineering, an introduction. New York: Wiley; 2003.
[6] Tibbetts GG, Beetz CP. Mechanical-properties of vapor-grown carbon-fibers. J Phys D—Appl Phys 1987;20(3):292–7.
[7] Hata K, Futaba DN, Mizuno K, Namai T, Yumura M, Iijima S. Water-assisted highly efficient synthesis of impurity-free single-walled carbon nanotubes. Science 2004;306(5700):1362–4.
[8] Wong EW, Sheehan PE, Lieber CM. Nanobeam mechanics: elasticity, strength, and toughness of nanorods and nanotubes. Science 1997;277:1971–5.
[9] Yu M, Lourie O, Dyer MJ, Kelly TF, Ruoff RS. Strength and breaking mechanism of multiwalled carbon nanotubes under tensile load. Science 2000;287:637–40.
[10] Xie S, Li W, Pan Z, Chang B, Sun L. Mechanical and physical properties on carbon nanotube. J Phys Chem Solids 2000;61(7):1153–8.
[11] Bethune DS, Kiang CH, Devries MS, Gorman G, Savoy R, Vazquez J, et al. Cobalt-catalyzed growth of carbon nanotubes with single-atomic-layerwalls. Nature 1993;363(6430):605–7.
[12] Iijima S, Ichihashi T. Single-shell carbon nanotubes of 1-nm diameter. Nature 1993;363(6430):603–5.
[13] Iijima S. Helical microtubules of graphitic carbon. Nature 1991;354(6348):56–8.
[14] Puretzky AA, Geohegan DB, Fan X, Pennycook SJ. In situ imaging and spectroscopy of single-wall carbon nanotube synthesis by laser vaporization. Appl Phys Lett 2000;76(2):182–4.
[15] Hernadi K, Fonseca A, Nagy JB, Bernaerts D, Fudala A, Lucas AA. Catalytic synthesis of carbon nanotubes using zeolite support. Zeolites 1996;17(5–6):416–23.
[16] Che G, Lakshmi BB, Martin CR, Fisher ER, Ruoff RS. Chemical vapor deposition based synthesis of carbon nanotubes and nanofibers using a template method. Chem Mater 1998;10(11):260–7.
[17] Zhou W, Ooi YH, Russo R, Papanek P, Luzzi DE, Fischer JE, et al. Structural characterization and diameter-dependent oxidative stability of single wall carbon nanotubes synthesized by the catalytic decomposition of CO. Chem Phys Lett 2001;350(1–2):6–14.
[18] Elliott JA, Sandler JKW, Windle AH, Young RJ, Shaffer MSP. Collapse of single-wall carbon nanotubes is diameter dependent. Phys Rev Lett 2004;92(9):1–4.
[19] Wei BQ, Vajtai R, Ajayan PM. Reliability and current carrying capacity of carbon nanotubes. Appl Phys Lett 2001;79(8): 1172–4.
[20] Kim BM, Fuhrer AMS. Properties and applications of high-mobility semiconducting nanotubes. J Phys: Condens Matter 2004;16(18):R553–80.
[21] Tang ZK, Zhang LY, Wang N, Zhang XX, Wen GH, Li GD, et al. Superconductivity in 4 Angstrom single-walled carbon nanotubes. Science 2001;292(5526):2462–5.
[22] Che JW, Cagin T, Goddard WA. Thermal conductivity of carbon nanotubes. Nanotechnology 2000;11(2):65–9.
[23] Osman MA, Srivastava D. Temperature dependence of the thermal conductivity of single-wall carbon nanotubes. Nanotechnology 2001;12(1):21–4.
[24] Berber S, Kwon Y, Tománek D. Unusually high thermal conductivity of carbon nanotubes. Phys Rev Lett 2000;84(20):4613–6.
[25] Hone J, Llaguno MC, Biercuk MJ, Johnson AT, Batlogg B, Benes Z, et al. Thermal properties of carbon nanotubes and nanotube-based materials. Appl Phys A—Mater Sci Process 2002;74(3): 339–43.
[26] Cadek M, Murphy R, McCarthy B, Drury A, Lahr B, Barklie RC, et al. Optimisation of the arc-discharge production of multi-walled carbon nanotubes. Carbon 2002;40(6):923–8.
[27] Frank S, Poncharal P, Wang ZL, de Heer WA. Carbon nanotube quantum resistors. Science 1998;280(5370):1744–6.
[28] Kim P, Shi L, Majumdar A, McEuen PL. Thermal transport measurements of individual multiwalled nanotubes. Phys Rev Lett 2001;87:215502–6606.
[29] Kelly BT. Physics of graphite. London: Applied Science; 1981.
[30] Kelly A, Macmillan NH. Strong solids. Oxford University Press; 1986.
[31] Bacon R. Growth, structure, and properties of graphite whiskers. J Appl Phys 1960;31(2):283–90.
[32] Overney G, Zhong W, Tomanek D. Structural rigidity and low-frequency vibrational-modes of long carbon tubules. Z Phys D—At Mol Clusters 1993;27(1):93–6.
[33] Lu JP. Elastic properties of single and multilayered nanotubes. J Phys Chem Solids 1997;58(11):1649–52.

[34] Treacy MMJ, Ebbesen TW, Gibson JM. Exceptionally high Young's modulus observed for individual carbon nanotubes. Nature 1996;381(6584):678–80.
[35] Poncharal P, Wang ZL, Ugarte D, de Heer WA. Electrostatic deflections and electromechanical resonances of carbon nanotubes. Science 1999;283(5407):1513–6.
[36] Falvo MR, Clary GJ, Taylor RM, Chi V, Brooks FP, Washburn S, et al. Bending and buckling of carbon nanotubes under large strain. Nature 1997;389(6651):582–4.
[37] Salvetat JP, Kulik AJ, Bonard JM, Briggs GAD, Stockli T, Metenier K, et al. Elastic modulus of ordered and disordered multiwalled carbon nanotubes. Adv Mater 1999;11(2):161–5.
[38] Salvetat JP, Briggs GAD, Bonard JM, Bacsa RR, Kulik AJ, Stockli T, et al. Elastic and shear moduli of single-walled carbon nanotube ropes. Phys Rev Lett 1999;82(5):944–7.
[39] Yu MF, Files BS, Arepalli S, Ruoff RS. Tensile loading of ropes of single wall carbon nanotubes and their mechanical properties. Phys Rev Lett 2000;84(24):5552–5.
[40] Miko C, Milas M, Seo JW, Couteau E, Barisic N, Gaal R, et al. Effect of electron irradiation on the electrical properties of fibers of aligned single-walled carbon nanotubes. Appl Phys Lett 2003;83(22): 4622–4.
[41] Kis A, Csanyi G, Salvetat JP, Lee TN, Couteau E, Kulik AJ, et al. Reinforcement of single-walled carbon nanotube bundles by intertube bridging. Nat Mater 2004;3(3):153–7.
[42] Tucker CL, Liang E. Stiffness predictions for unidirectional short-fiber composites: review and evaluation. Compos Sci Technol 1999; 59(5):655–71.
[43] Kelly A, Tyson WR. Tensile properties of fibre-reinforced metals—copper/tungsten and copper/molybdenum. J Mech Phys Solids 1965; 13(6):329–50.
[44] Cox HL. The elasticity and strength of paper and other fibrous materials. Br J Appl Phys 1952;3:72–9.
[45] Carman GP, Reifsnider KL. Micromechanics of short-fiber composites. Compos Sci Technol 1992;43(2):137–46.
[46] Krenchel H. Fibre reinforcement. Copenhagen: Akademisk Forlag; 1964.
[47] Cooper CA, Cohen SR, Barber AH, Wagner HD. Detachment of nanotubes from a polymer matrix. Appl Phys Lett 2002;81(20): 3873–5.
[48] Coleman JN, Cadek M, Blake R, Nicolosi V, Ryan KP, Belton C, et al. High performance nanotube-reinforced plastics: understanding the mechanism of strength increase. Adv Funct Mater 2004; 14(8):791–8.
[49] Halpin JC, Kardos JL. The Halpin–Tsai equations: a review. Polym Eng Sci 1976;16(5):344–52.
[50] Hill R. Theory of mechanical properties of fibre-strengthened materials: I. Elastic behaviour. J Mech Phys Solids 1964;12(4): 199–212.
[51] Manchado MAL, Valentini L, Biagiotti J, Kenny JM. Thermal and mechanical properties of single-walled carbon nanotubes-polypropylene composites prepared by melt processing. Carbon 2005;43(7): 1499–505.
[52] Ajayan PM, Schadler LS, Giannaris C, Rubio A. Single-walled carbon nanotube–polymer composites: strength and weakness. Adv Mater 2000;12(10):750–3.
[53] Schadler LS, Giannaris SC, Ajayan PM. Load transfer in carbon nanotube epoxy composites. Appl Phys Lett 1998;73(26):3842–4.
[54] Ruan SL, Gao P, Yang XG, Yu TX. Toughening high performance ultrahigh molecular weight polyethylene using multiwalled carbon nanotubes. Polymer 2003;44(19):5643–54.
[55] Cooper CA, Young RJ, Halsall M. Investigation into the deformation of carbon nanotubes and their composites through the use of Raman spectroscopy. Compos Part A: Appl Sci Manuf 2001; 32(3–4):401–11.
[56] Frankland SJV, Caglar A, Brenner DW, Griebel M. Molecular simulation of the influence of chemical cross-links on the shear strength of carbon nanotube–polymer interfaces. J Phys Chem B 2002;106(12):3046–8.
[57] Liao K, Li S. Interfacial characteristics of a carbon nanotube–polystyrene composite system. Appl Phys Lett 2001;79(25):4225–7.
[58] Wong M, Paramsothy M, Xu XJ, Ren Y, Li S, Liao K. Physical interactions at carbon nanotube–polymer interface. Polymer 2003;44(25):7757–64.
[59] Lordi V, Yao N. Molecular mechanics of binding in carbon-nanotube–polymer composites. J Mater Res 2000;15(12):2770–9.
[60] Homola AM, Israelachvili JN, Gee ML, McGuiggan PM. Measurements of and relation between the adhesion and friction of 2 surfaces separated by molecularly thin liquid-films. J Tribol—Trans ASME 1989;111(4):675–82.
[61] Wall A, Coleman JN, Ferreira MS. Physical mechanism for the mechanical reinforcement in nanotube–polymer composite materials. Phys Rev B 2005;71:125421–6.
[62] Wagner HD, Lourie O, Feldman Y, Tenne R. Stress-induced fragmentation of multiwall carbon nanotubes in a polymer matrix. Appl Phys Lett 1998;72(2):188–90.
[63] Barber AH, Cohen SR, Wagner HD. Measurement of carbon nanotube–polymer interfacial strength. Appl Phys Lett 2003;82(23): 4140–2.
[64] Barber AH, Cohen SR, Kenig S, Wagner HD. Interfacial fracture energy measurements for multi-walled carbon nanotubes pulled from a polymer matrix. Compos Sci Technol 2004;64(15):2283–9.
[65] Yang M, Koutsos V, Zaiser M. Interactions between polymers and carbon nanotubes: a molecular dynamics study. J Phys Chem B 2005;109(20):10009–14.
[66] McCarthy B, Coleman JN, Czerw R, Dalton AB, in het Panhuis M, Maiti A, et al. A microscopic and spectroscopic study of interactions between carbon nanotubes and a conjugated polymer. J Phys Chem B 2002;106(9):2210–6.
[67] McCarthy B, Coleman JN, Curran SA, Dalton AB, Davey AP, Konya Z, et al. Observation of site selective binding in a polymer nanotube composite. J Mater Sci Lett 2000;19(24):2239–41.
[68] Coleman JN, Ferreira MS. Geometric constraints in the growth of nanotube-templated polymer monolayers. Appl Phys Lett 2004; 84(5):798–800.
[69] Wei C, Srivastava D, Cho K. Structural ordering in nanotube polymer composites. Nano Letters 2004;4(10):1949–52.
[70] Ding W, Eitan A, Fisher FT, Chen X, Dikin DA, Andrews R, et al. Direct observation of polymer sheathing in carbon nanotube–polycarbonate composites. Nano Letters 2003;3(11):1593–7.
[71] Potschke P, Fornes TD, Paul DR. Rheological behavior of multiwalled carbon nanotube/polycarbonate composites. Polymer 2002;43(11):3247–55.
[72] Assouline E, Lustiger A, Barber AH, Cooper CA, Klein E, Wachtel E, et al. Nucleation ability of multiwall carbon nanotubes in polypropylene composites. J Polym Sci Part B: Polym Phys 2003; 41(5):520–7.
[73] Xie XL, Aloys K, Zhou XP, Zeng FD. Ultrahigh molecular mass polyethylene/carbon nanotube composites—crystallization and melting properties. J Therm Anal Calorim 2003;74(1):317–23.
[74] Sandler J, Broza G, Nolte M, Schulte K, Lam YM, Shaffer MSP. Crystallization of carbon nanotube and nanofiber polypropylene composites. J Macromol Sci—Phys 2003;B42(3–4):479–88.
[75] Grady BP, Pompeo F, Shambaugh RL, Resasco DE. Nucleation of polypropylene crystallization by single-walled carbon nanotubes. J Phys Chem B 2002;106(23):5852–8.
[76] Wu C-M, Chen M, Karger-Kocsis J. Interfacial shear strength and failure modes in sPP/CF and iPP/CF microcomposites by fragmentation. Polymer 2001;42(1):129–35.
[77] Jin L, Bower C, Zhou O. Alignment of carbon nanotubes in a polymer matrix by mechanical stretching. Appl Phys Lett 1998;73(9):1197–9.
[78] Shaffer MSP, Windle AH. Fabrication and characterization of carbon nanotube/poly(vinyl alcohol) composites. Adv Mater 1999; 11(11):937–41.
[79] Qian D, Dickey EC, Andrews R, Rantell T. Load transfer and deformation mechanisms in carbon nanotube–polystyrene composites. Appl Phys Lett 2000;76(20):2868–70.

[80] Safadi B, Andrews R, Grulke EA. Multiwalled carbon nanotube polymer composites: synthesis and characterization of thin films. J Appl Polym Sci 2002;84(14):2660–9.
[81] Velasco-Santos C, Martinez-Hernandez AL, Fisher F, Ruoff R, Castano VM. Dynamical-mechanical and thermal analysis of carbon nanotube–methyl–ethyl methacrylate nanocomposites. J Phys D—Appl Phys 2003;36(12):1423–8.
[82] Dufresne A, Paillet M, Putaux JL, Canet R, Carmona F, Delhaes P, et al. Processing and characterization of carbon nanotube/poly(styrene-co-butyl acrylate) nanocomposites. J Mater Sci 2002;37(18):3915–23.
[83] Probst O, Moore EM, Resasco DE, Grady BP. Nucleation of polyvinyl alcohol crystallization by single-walled carbon nanotubes. Polymer 2004;45(13):4437–43.
[84] Dalmas F, Chazeau L, Gauthier C, Masenelli-Varlot K, Dendievel R, Cavaillé JY, et al. Multiwalled carbon nanotube/polymer nanocomposites: processing and properties. J Polym Sci Part B: Polym Phys 2005;43(10):1186–97.
[85] Watts PCP, Hsu WK. Behaviours of embedded carbon nanotubes during film cracking. Nanotechnology 2003(5):L7–L10.
[86] Cadek M, Coleman JN, Ryan KP, Nicolosi V, Bister G, Fonseca A, et al. Reinforcement of polymers with carbon nanotubes: the role of nanotube surface area. Nano Letters 2004;4(2):353–6.
[87] Cadek M, Coleman JN, Barron V, Hedicke K, Blau WJ. Morphological and mechanical properties of carbon-nanotube-reinforced semicrystalline and amorphous polymer composites. Appl Phys Lett 2002;81(27):5123–5.
[88] Andrews R, Jacques D, Minot M, Rantell T. Fabrication of carbon multiwall nanotube/polymer composites by shear mixing. Macromol Mater Eng 2002;287(6):395–403.
[89] Breuer O, Sundararaj U. Big returns from small fibers: a review of polymer/carbon nanotube composites. Polym Compos 2004;25(6):630–45.
[90] Potschke P, Bhattacharyya AR, Janke A, Goering H. Melt mixing of polycarbonate/multi-wall carbon nanotube composites. Compos Interf 2003;10(4–5):389–404.
[91] Jin Z, Pramoda K, Xu G, Goh SH. Dynamic mechanical behavior of melt-processed multi-walled carbon nanotube/poly(methyl methacrylate) composites. Chem Phys Lett 2001;337(1–3):43–7.
[92] Andrews R, Jacques D, Qian DL, Rantell T. Multiwall carbon nanotubes: synthesis and application. Acc Chem Res 2002;35(12):1008–17.
[93] Liu TX, Phang IY, Shen L, Chow SY, Zhang W-D. Morphology and mechanical properties of multiwalled carbon nanotubes reinforced nylon-6 composites. Macromolecules 2004;37(19):7214–22.
[94] De Zhang W, Shen L, Phang IY, Liu TX. Carbon nanotubes reinforced nylon-6 composite prepared by simple melt-compounding. Macromolecules 2004;37(2):256–9.
[95] Gorga RE, Cohen RE. Toughness enhancements in poly(methyl methacrylate) by addition of oriented multiwall carbon nanotubes. J Polym Sci Part B: Polym Phys 2004;42(14):2690–702.
[96] Meincke O, Kaempfer D, Weickmann H, Friedrich C, Vathauer M, Warth H. Mechanical properties and electrical conductivity of carbon-nanotube filled polyamide-6 and its blends with acrylonitrile/butadiene/styrene. Polymer 2004;45(3):739–48.
[97] Tang W, Santare MH, Advani SG. Melt processing and mechanical property characterization of multi-walled carbon nanotube/high density polyethylene (MWNT/HDPE) composite films. Carbon 2003;41(14):2779–85.
[98] Thostenson ET, Chou T-W. Aligned multi-walled carbon nanotube-reinforced composites: processing and mechanical characterization. J Phys D: Appl Phys 2002(16):L77–80.
[99] Cooper CA, Ravich D, Lips D, Mayer J, Wagner HD. Distribution and alignment of carbon nanotubes and nanofibrils in a polymer matrix. Compos Sci Technol 2002;62(7–8):1105–12.
[100] Haggenmueller R, Gommans HH, Rinzler AG, Fischer JE, Winey KI. Aligned single-wall carbon nanotubes in composites by melt processing methods. Chem Phys Lett 2000;330(3–4):219–25.
[101] Kearns JC, Shambaugh RL. Polypropylene fibers reinforced with carbon nanotubes. J Appl Polym Sci 2002;86(8):2079–84.
[102] Moore EM, Ortiz DL, Marla VT, Shambaugh RL, Grady BP. Enhancing the strength of polypropylene fibers with carbon nanotubes. J Appl Polym Sci 2004;93(6):2926–33.
[103] Sandler JKW, Pegel S, Cadek M, Gojny F, van Es M, Lohmar J, et al. A comparative study of melt spun polyamide-12 fibres reinforced with carbon nanotubes and nanofibres. Polymer 2004;45(6):2001–15.
[104] Li QQ, Zaiser M, Koutsos V. Carbon nanotube/epoxy resin composites using a block copolymer as a dispersing agent. Phys Status Solidi a—Appl Res 2004;201(13):R89–91.
[105] Lau K-t, Lu M, Chun-ki Lam, Cheung H-y, Sheng F-L, Li H-L. Thermal and mechanical properties of single-walled carbon nanotube bundle-reinforced epoxy nanocomposites: the role of solvent for nanotube dispersion. Compos Sci Technol 2005;65(5):719–25.
[106] Xu X, Thwe MM, Shearwood C, Liao K. Mechanical properties and interfacial characteristics of carbon-nanotube–reinforced epoxy thin films. Appl Phys Lett 2002;81(15):2833–5.
[107] Ogasawara T, Ishida Y, Ishikawa T, Yokota R. Characterization of multi-walled carbon nanotube/phenylethynyl terminated polyimide composites. Compos Part A: Appl Sci Manuf 2004;35(1):67–74.
[108] Coleman JN, Blau WJ, Dalton AB, Munoz E, Collins S, Kim BG, et al. Improving the mechanical properties of single-walled carbon nanotube sheets by intercalation of polymeric adhesives. Appl Phys Lett 2003;82(11):1682–4.
[109] Wang Z, Liang Z, Wang B, Zhang C, Kramer L. Processing and property investigation of single-walled carbon nanotube (SWNT) Buckypaper/epoxy resin matrix nanocomposites. Compos Part A: Appl Sci Manuf 2004;35(10):1225–32.
[110] Lahiff E, Ryu CY, Curran S, Minett AI, Blau WJ, Ajayan PM. Selective positioning and density control of nanotubes within a polymer thin film. Nano Letters 2003;3(10):1333–7.
[111] Mamedov AA, Kotov NA, Prato M, Guldi DM, Wicksted JP, Hirsch A. Molecular design of strong single-wall carbon nanotube/polyelectrolyte multilayer composites. Nat Mater 2002;1(3):190–4.
[112] Olek M, Ostrander J, Jurga S, Mohwald H, Kotov N, Kempa K, et al. Layer-by-layer assembled composites from multiwall carbon nanotubes with different morphologies. Nano Letters 2004;4(10):1889–95.
[113] Qin S, Qin D, Ford WT, Zhang Y, Kotov NA. Covalent cross-linked polymer/single-wall carbon nanotube multilayer films. Chem Mater 2005;17(8):2131–5.
[114] Vigolo B, Penicaud A, Coulon C, Sauder C, Pailler R, Journet C, et al. Macroscopic fibers and ribbons of oriented carbon nanotubes. Science 2000;290(5495):1331–4.
[115] Dalton AB, Collins S, Munoz E, Razal JM, Ebron VH, Ferraris JP, et al. Super-tough carbon-nanotube fibres—these extraordinary composite fibres can be woven into electronic textiles. Nature 2003;423(6941):703.
[116] Miaudet P, Badaire S, Maugey M, Derre A, Pichot V, Launois P, et al. Hot-drawing of single and multiwall carbon nanotube fibers for high toughness and alignment. Nano Letters 2005;5(11):2212–5.
[117] Formhals A. Inventor electrical spinning of fibers from solutions. United States Patent 2,123,992, 1934.
[118] Ko F, Gogotsi Y, Ali A, Naguib N, Ye HH, Yang GL, et al. Electrospinning of continuous carbon nanotube-filled nanofiber yarns. Adv Mater 2003;15(14):1161–5.
[119] Sen R, Zhao B, Perea D, Itkis ME, Hu H, Love J, et al. Preparation of single-walled carbon nanotube reinforced polystyrene and polyurethane nanofibers and membranes by electrospinning. Nano Letters 2004;4(3):459–64.
[120] Jia Z, Wang Z, Xu C, Liang J, Wei B, Wu D, et al. Study on poly(methyl methacrylate)/carbon nanotube composites. Mater Sci Eng A 1999;271(1–2):395–400.
[121] Velasco-Santos C, Martinez-Hernandez AL, Fisher FT, Ruoff R, Castano VM. Improvement of thermal and mechanical properties of

carbon nanotube composites through chemical functionalization. Chem Mater 2003;15(23):4470–5.
[122] Putz KW, Mitchell CA, Krishnamoorti R, Green PF. Elastic modulus of single-walled carbon nanotube/poly(methyl methacrylate) nanocomposites. J Polym Sci Part B: Polym Phys 2004;42(12):2286–93.
[123] Kumar S, Dang TD, Arnold FE, Bhattacharyya AR, Min BG, Zhang X, et al. Synthesis, structure, and properties of PBO/SWNT composites. Macromolecules 2002;35(24):9039–43.
[124] Zhao C, Hu G, Justice R, Schaefer DW, Zhang S, Yang M, et al. Synthesis and characterization of multi-walled carbon nanotubes reinforced polyamide 6 via in situ polymerization. Polymer 2005;46(14):5125–32.
[125] Gao J, Itkis ME, Yu A, Bekyarova E, Zhao B, Haddon RC. Continuous spinning of a single-walled carbon nanotube–nylon composite fiber. J Am Chem Soc 2005;127(11):3847–54.
[126] Park C, Ounaies Z, Watson KA, Crooks RE, Joseph SJ, Lowther SE, et al. Dispersion of single wall carbon nanotubes by in situ polymerization under sonication. Chem Phys Lett 2002;364(3–4):303–8.
[127] Zhu J, Kim J, Peng H, Margrave JL, Khabashesku VN, Barrera EV. Improving the dispersion and integration of single-walled carbon nanotubes in epoxy composites through functionalization. Nano Letters 2003;3(8):1107–13.
[128] Zhu J, Peng H, Rodriguez-Macias F, Margrave JL, Khabashesku VN, Imam AM, et al. Reinforcing epoxy polymer composites through covalent integration of functionalized nanotubes. Adv Funct Mater 2004;14(7):643–8.
[129] Stevens JL, Huang AY, Peng H, Chiang IW, Khabashesku VN, Margrave JL. Sidewall amino-functionalization of single-walled carbon nanotubes through fluorination and subsequent reactions with terminal diamines. Nano Letters 2003;3(3):331–6.
[130] Gojny FH, Schulte K. Functionalisation effect on the thermo-mechanical behaviour of multi-wall carbon nanotube/epoxy-composites. Compos Sci Technol 2004;64(15):2303–8.
[131] Banerjee S, Hemraj-Benny T, Wong SS. Covalent surface chemistry of single-walled carbon nanotubes. Adv Mater 2005;17(1):17–29.
[132] Garg A, Sinnott SB. Effect of chemical functionalization on the mechanical properties of carbon nanotubes. Chem Phys Lett 1998;295(4):273–8.
[133] Viswanathan G, Chakrapani N, Yang H, Wei B, Chung H, Cho K, et al. Single-step in situ synthesis of polymer-grafted single-wall nanotube composites. J Am Chem Soc 2003;125(31):9258–9.
[134] Qin S, Qin D, Ford WT, Resasco DE, Herrera JE. Functionalization of single-walled carbon nanotubes with polystyrene via grafting to and grafting from methods. Macromolecules 2004;37(3):752–7.
[135] Hwang GL, Shieh Y-T, Hwang KC. Efficient load transfer to polymer-grafted multiwalled carbon nanotubes in polymer composites. Adv Funct Mater 2004;14(5):487–91.
[136] Xia H, Wang Q, Qiu G. Polymer-encapsulated carbon nanotubes prepared through ultrasonically initiated in situ emulsion polymerization. Chem Mater 2003;15(20):3879–86.
[137] Tong X, Liu C, Cheng H-M, Zhao H, Yang F, Zhang X. Surface modification of single-walled carbon nanotubes with polyethylene via in situ Ziegler–Natta polymerization. J Appl Polym Sci 2004;92(6):3697–700.
[138] Fu K, Huang W, Lin Y, Riddle LA, Carroll DL, Sun YP. Defunctionalization of functionalized carbon nanotubes. Nano Letters 2001;1(8):439–41.
[139] Lou X, Detrembleur C, Sciannamea V, Pagnoulle C, Jerome R. Grafting of alkoxyamine end-capped (co)polymers onto multi-walled carbon nanotubes. Polymer 2004;45(18):6097–102.
[140] Bhattacharyya S, Sinturel C, Salvetat JP, Saboungi M-L. Protein-functionalized carbon nanotube–polymer composites. Appl Phys Lett 2005;86(11):113104–6.
[141] Liu L, Barber AH, Nuriel S, Wagner HD. Mechanical properties of functionalized single-walled carbon-nanotube/poly(vinyl alcohol) nanocomposites. Adv Funct Mater 2005;15(6):975–80.
[142] Blake R, Gun'ko YK, Coleman J, Cadek M, Fonseca A, Nagy JB, et al. A generic organometallic approach toward ultra-strong carbon nanotube polymer composites. J Am Chem Soc 2004;126(33):10226–7.
[143] Yang J, Hu J, Wang C, Qin Y, Guo Z. Fabrication and characterization of soluble multi-walled carbon nanotubes reinforced P(MMA-co-EMA) composites. Macromol Mater Eng 2004;289(9):828–32.
[144] Broza G, Kwiatkowska M, Roslaniec Z, Schulte K. Processing and assessment of poly(butylene terephthalate) nanocomposites reinforced with oxidized single wall carbon nanotubes. Polymer 2005;46(16):5860–7.
[145] Lourie O, Wagner HD. Evaluation of Young's modulus of carbon nanotubes by micro-Raman spectroscopy. J Mater Res 1998;13:2418–23.
[146] Chang TE, Jensen LR, Kisliuk A, Pipes RB, Pyrz R, Sokolov AP. Microscopic mechanism of reinforcement in single-wall carbon nanotube/polypropylene nanocomposite. Polymer 2005;46(2):439–44.
[147] Ajayan PM, Stephan O, Colliex C, Trauth D. Aligned carbon nanotube arrays formed by cutting a polymer resin–nanotube composite. Science 1994;265(5176):1212–4.
[148] Allaoui A, Bai S, Cheng HM, Bai JB. Mechanical and electrical properties of a MWNT/epoxy composite. Compos Sci Technol 2002;62(15):1993–8.
[149] Breton Y, Desarmot G, Salvetat JP, Delpeux S, Sinturel C, Beguin F, et al. Mechanical properties of multiwall carbon nanotubes/epoxy composites: influence of network morphology. Carbon 2004;42(5–6):1027–30.
[150] Bai J. Evidence of the reinforcement role of chemical vapour deposition multi-walled carbon nanotubes in a polymer matrix. Carbon 2003;41(6):1325–8.
[151] Li XD, Gao HS, Scrivens WA, Fei DL, Xu XY, Sutton MA, et al. Nanomechanical characterization of single-walled carbon nanotube reinforced epoxy composites. Nanotechnology 2004;15(11):1416–23.
[152] Ward IM, Sweeney J. The mechanical properties of solid polymers. Wiley; 2004.
[153] Frizzell CJ, in het Panhuis M, Countinho DH, Balkus Jr KJ, Minett AI, Blau WJ, et al. Reinforcement of macroscopic carbon nanotube structures by polymer intercalation: the role of polymer molecular weight and chain conformation. Phys Rev B 2005;72:1–8.
[154] Lahiff E, Leahy R, Coleman JN, Blau WJ. Physical properties of novel free-standing polymer–nanotube thin films. Carbon 2006;44(8):1525–9.
[155] Li Y-L, Kinloch IA, Windle AH. Direct spinning of carbon nanotube fibers from chemical vapor deposition synthesis. Science 2004;304(5668):276–8.
[156] Zhang M, Atkinson KR, Baughman RH. Multifunctional carbon nanotube yarns by downsizing an ancient technology. Science 2004;306(5700):1358–61.
[157] Zhang M, Fang S, Zakhidov AA, Lee SB, Aliev AE, Williams CD, et al. Strong, transparent, multifunctional, carbon nanotube sheets. Science 2005;309(5738):1215–9.
[158] Vigolo B, Poulin P, Lucas M, Launois P, Bernier P. Improved structure and properties of single-wall carbon nanotube spun fibers. Appl Phys Lett 2002;81(7):1210–2.
[159] Dalton AB, Collins S, Razal J, Munoz E, Ebron VH, Kim BG, et al. Continuous carbon nanotube composite fibers: properties, potential applications, and problems. J Mater Chem 2004;14(1):1–3.
[160] Munoz E, Dalton AB, Collins S, Kozlov M, Razal J, Coleman JN, et al. Multifunctional carbon nanotube composite fibers. Adv Eng Mater 2004;6(10):801–4.
[161] Barisci JN, Tahhan M, Wallace GG, Badaire S, Vaugien T, Maugey M, et al. Properties of carbon nanotube fibers spun from DNA-stabilized dispersions. Adv Funct Mater 2004;14(2):133–8.
[162] Shaffer M, Kinloch IA. Prospects for nanotube and nanofibre composites. Compos Sci Technol 2004;64(15):2281–2.